Behavioral/Systems/Cognitive

Associative Learning and CA3–CA1 Synaptic Plasticity Are Impaired in D_1R Null, *Drd1a*$^{-/-}$ Mice and in Hippocampal siRNA Silenced *Drd1a* Mice

Oskar Ortiz,[1,2] José María Delgado-García,[3] Isabel Espadas,[1,2] Amine Bahí,[4] Ramón Trullas,[2,5] Jean-Luc Dreyer,[4] Agnès Gruart,[3]* and Rosario Moratalla[1,2]*

[1]Instituto Cajal, Consejo Superior de Investigaciones Científicas (CSIC), Madrid 28002, Spain, [2]Centro de Investigación Biomédica en Red sobre Enfermedades Neurodegenerativas, Instituto de Salud Carlos III, Madrid 28002, Spain, [3]División de Neurociencias, Universidad Pablo de Olavide, Sevilla 41013, Spain, [4]University of Fribourg, Fribourg, Switzerland, and [5]Instituto de Invest Biomédicas de Barcelona, CSIC, Barcelona 08036, Spain

Associative learning depends on multiple cortical and subcortical structures, including striatum, hippocampus, and amygdala. Both glutamatergic and dopaminergic neurotransmitter systems have been implicated in learning and memory consolidation. While the role of glutamate is well established, the role of dopamine and its receptors in these processes is less clear. In this study, we used two models of dopamine D_1 receptor (D_1R, *Drd1a*) loss, D_1R knock-out mice (*Drd1a*$^{-/-}$) and mice with intrahippocampal injections of *Drd1a*-siRNA (small interfering RNA), to study the role of D_1R in different models of learning, hippocampal long-term potentiation (LTP) and associated gene expression. D_1R loss markedly reduced spatial learning, fear learning, and classical conditioning of the eyelid response, as well as the associated activity-dependent synaptic plasticity in the hippocampal CA1–CA3 synapse. These results provide the first experimental demonstration that D_1R is required for trace eyeblink conditioning and associated changes in synaptic strength in hippocampus of behaving mice. *Drd1a*-siRNA mice were indistinguishable from *Drd1a*$^{-/-}$ mice in all experiments, indicating that hippocampal knockdown was as effective as global inactivation and that the observed effects are caused by loss of D_1R and not by indirect developmental effects of *Drd1a*$^{-/-}$. Finally, *in vivo* LTP and LTP-induced expression of *Egr1* in the hippocampus were significantly reduced in *Drd1a*$^{-/-}$ and *Drd1a*-siRNA, indicating an important role for D_1R in these processes. Our data reveal a functional relationship between acquisition of associative learning, increase in synaptic strength at the CA3–CA1 synapse, and *Egr1* induction in the hippocampus by demonstrating that all three are dramatically impaired when D_1R is eliminated or reduced.

Introduction

Recent studies demonstrate that dopamine plays an important role in learning and memory. Moreover, integration of glutamate- and dopamine-mediated signals at the cellular level is required for persistent long-term potentiation (LTP) (O'Carroll and Morris, 2004), learning (Smith-Roe and Kelley, 2000; Baldwin et al., 2002), and long-term memory (O'Carroll et al., 2006). Exposure to a novel environment facilitates LTP (Li et al., 2003), linking dopamine signaling with enhanced LTP and with new information acquisition and storage (Lisman and Grace, 2005). Conversely, dopaminergic dysfunction significantly alters spatial learning and short- and long-term memory in rodents and in nonhuman primates (Whishaw and Dunnett, 1985; Williams and Goldman-Rakic, 1995). Dopamine depletion causes cognitive deficits in Parkinson's disease patients (Dubois and Pillon, 1997; Levin and Katzen, 2005), in agreement with studies in dopamine-deficient mice (Palmiter, 2008; Darvas and Palmiter, 2009), stressing the importance of dopamine in learning and associated synaptic plasticity.

The dopamine D_1 receptor (D_1R), in particular, has been implicated in mediating dopamine's effects in learning and synaptic plasticity. Pharmacological blockade of D_1/D_5 receptors significantly diminishes early and late phases of LTP in rat hippocampal slices (Otmakhova and Lisman, 1996) and blocks long-term memory storage (O'Carroll et al., 2006; Rossato et al., 2009) *in vivo*. Selective genetic inactivation of the dopamine D_1R subtype (*Drd1a*) differentiated between the roles of D_1 and D_5 receptor subtypes in LTP (Granado et al., 2008) and spatial learning (El-Ghundi et al., 1999; Granado et al., 2008). However, the role of the D_1R in associative learning and classical conditioning is less clear, as is its role in the synaptic changes that occur in hippocampal networks *in vivo* during the acquisition of new information. Most, if not all, of the electrophysiological studies involving D_1R have been performed *in vitro*.

Trace eyeblink conditioning, a form of associative learning, was recently shown to induce a progressive increase in strength at the hippocampal CA3–CA1 synapse in awake mice (Gruart et al.,

Received May 25, 2010; revised July 7, 2010; accepted July 20, 2010.

This work was supported by Grant PI071073 from Plan Nacional Sobre Drogas from the Spanish Ministerio de Sanidad y Política Social and Spanish Ministerio de Ciencia e Innovación Grants BFU2010-20664 (R.M.) and BFU2005-01024 and BFU2005-02512 (J.M.D.-G. and A.G.). O.O. was supported by a Basque Government Ph.D. fellowship. We thank M. Esteban, E. Rubio, and M. de Mesa for technical assistance and Dr. Angel Barco for help and advice with the fear-conditioning test.

*A.G. and R.M. contributed equally to this work.

Correspondence should be addressed to Dr. Rosario Moratalla, Instituto Cajal, Consejo Superior de Investigaciones Científicas, Avda Dr Arce, 37, Madrid, Spain. E-mail: moratalla@cajal.csic.es.

DOI:10.1523/JNEUROSCI.2655-10.2010

 0270-6474/10/3012288-13$15.00/0

2006; Madroñal et al., 2009) that correlates with the progressive increase in conditioned responses. To directly demonstrate the relationship between LTP and associative learning, we studied the role of D_1R in associative learning and synaptic plasticity in adult behaving mice. LTP is well established as a form of synaptic memory but is usually studied under nonphysiological conditions. Our approach here is unique in that we simultaneously assess trace eyeblink conditioning and synaptic efficiency by measuring changes in evoked extracellular field EPSPs (fEPSPs) at the CA3–CA1 synapse in behaving animals during conditioning. We compared wild-type (WT) mice to genetically engineered mice lacking D_1R (*Drd1a*$^{-/-}$). In addition, we used small interfering RNA (siRNA) technology to silence *Drd1a* in adult mice *in vivo*. Our data reveal a functional relationship between acquisition of associative learning, increase in synaptic strength at the CA3–CA1 synapse, and Egr1 expression in the hippocampus by revealing that all three are dramatically impaired when D_1R is eliminated or reduced. These results indicate an important role for hippocampal D_1R in associative learning and its physiological and molecular correlates.

Materials and Methods

Animals. All experiments were performed on 3- to 6-month-old (25–30 g) male mice. *Drd1a*$^{-/-}$ mice (Xu et al., 1994; Moratalla et al., 1996) were backcrossed to C57BL/6 for >10 generations. WT and *Drd1a*$^{-/-}$ mice used in this study were derived from the mating of heterozygous mice. Animal genotypes were determined by Southern blot analysis (Xu et al., 1994). RNA interference procedures were performed on WT C57BL/6 mice. Before surgery, animals were housed in separate cages ($n = 10$ per cage) on a 12 h light/dark cycle with constant ambient temperature (21 ± 1°C) and humidity (55 ± 9%). Food and water were available *ad libitum*. Electrophysiological and behavioral studies were performed in accordance with the guidelines of the European Union (2003/65/CE) and Spanish regulations (BOE 252/34367-91, 2005) for the use of laboratory animals in chronic experiments. Experiments were also approved by the local ethical committee.

Spatial learning: Barnes maze. In the Barnes maze, animals receive reinforcement to escape from the open platform surface to a small dark recessed chamber located under the platform called an "escape box." The paradigm consists of a circular platform (90 cm in diameter) with 20 holes (hole diameter, 5 cm) along the perimeter. Spatial cues were placed in the walls of the room during the experiment. The experiment was divided in three different phases. During the first 11 d, mice were trained to enter into the escape box; during the second part, mice rested for 3 d and were tested for long-term spatial memory. In the last phase, animals were trained again in the Barnes maze for 3 d, but the escape box was placed in a new position 180° from the original position. The task conditions during all phases were identical; the mouse was placed in the middle of the maze in a black cylindrical start. After 10 s elapsed, the cylinder was lifted, and the mouse was free to explore the maze. The trial ended when the mouse entered the escape box or after 2 min had elapsed; in this case, the mouse was guided to the escape box. In all cases, mice were allowed to stay 30 s in the escape box. All animals were given four training trials per day, and trials were separated by 20 min. After each trial, the maze was cleaned with 70% alcohol to eliminate the use of intramaze cues. Trials were recorded using a computerized tracking analyzer system (SMART, Panlab).

Active avoidance. For this test, we used a two-way shuttle box (Ugo Basile) with acrylic walls and stainless steel bars in the floor controlled by a programming/recording unit with a shock generator (Ugo Basile). Animals were given one training session each day for 7 consecutive days. Each training session consisted of an adaptation period of 3 min, in which animals were allowed to move freely from one compartment to the other, followed by 20 trials separated by an intertrial interval (ITI) of 20 s (±5 to counteract any time associations). In each trial, a white light and a tone (100 GHz, 100 dB) were presented simultaneously for 10 s in the compartment where the animal stayed and were used as the conditioned stimulus (CS). After 5 s of the CS, mice received a 0.2 mA electric footshock as the unconditioned stimulus (US) for a maximal duration of 10 s. An avoidance response was defined as when the animal crossed to the opposite compartment of the box after the CS started but before the US was delivered. Crossings while the shock was being delivered were considered escape responses. Response latencies were counted as the time (in seconds) from the onset of the CS until the animal crossed into the opposite compartment. The number of crosses during the ITI was determined as a measure of general activity. The test session was performed 3 d after the end of the training phase, on day 10 of the experiment. The apparatus was cleaned with water after each animal.

Passive avoidance. This test was performed as described previously (Pittenger et al., 2006). Mice were placed into the passive avoidance box (Ugo Basile) with two different compartments, one dark and black and the other illuminated and white. On the first test day, we measured how long the mice spent in the lighted compartment. As soon as the animal crossed to the dark compartment, the automatic door closed, and mice received an electrical footshock (0.4 or 0.8 mA, 1 s). At 1 and 24 h after this first trial with footshock, animals were tested in the box using the same conditions without the electrical shock.

Fear conditioning and extinction. This behavioral task was performed as described previously (Alarcón et al., 2004). On training day, mice were placed in the conditioning chamber for 2 min before onset of the CS, a 30 s tone. During the last 2 s of the tone, the US, an electrical shock of 0.7 mA, was presented. Mice were maintained in the chamber for an additional 30 s and returned to the home cage. Conditioning was tested 24 h later by measuring freezing behavior with a tracking video system (Panlab). Mice were re-placed into the conditioning chamber, and the freezing time was measured for 5 min without the tone to assess contextual conditioning. Mice were returned to home cages for 3 h and placed into a novel chamber to test cued fear conditioning. After 1 min in the novel context, the tone was presented for 30 s, and freezing time was measured for 2 min.

To study fear extinction, the US was modified to achieve equal freezing times in the two genotypes. The new US consisted of three consecutive electrical shocks (0.7 mA for 2 s, with 2 min intershock intervals) delivered in the conditioning chamber followed by a 2 min measurement of freezing time before returning animals to home cages. Extinction was assessed by measuring freezing for 5 min after the animals were re-placed in the same conditioning chamber, every day for 6 consecutive days.

Sensitivity to electric shock. This test was performed as described by El-Ghundi et al. (2001). Briefly, mice were subjected to a series of mild footshocks with gradually increasing amperage (0.02, 0.04, 0.06, 0.08, 0.1, 0.15, 0.2, 0.25, 0.3, 0.4, 0.5, 0.6 mA). Duration of footshock was 1 s with 20 s intershock intervals. For each mouse, we determined the shock intensity that produced each of the following initial sensation responses: sniffing and staring at the floor bars, licking and biting the floor bars, alternately lifting the paws off the floor, startle response, jumping, and vocalization.

Elevated plus maze. We used an apparatus with four 30 × 5 cm arms, elevated 50 cm above the floor (Cibertec). Two arms were enclosed by 15 cm walls, and the other two had a 3 mm edge to prevent slipping. All arms were illuminated equally. A 5 × 5 platform at the center was considered a neutral area. Animals were habituated to the experimenter, and 1 h before the experiment, animals were placed in the testing room. At the beginning of the test, animals were placed in the center of the maze facing the open arm and allowed to explore for 5 min. The percentage of time spent in the open arms compared with the total time minus time in the center as well as the number of entries to the open arms was used as the primary measure of anxiety-like behavior.

Nociceptive thresholds. We used three different nociceptive tests: hot plate, plantar, and tail immersion tests. We used the plantar test apparatus (Ugo Basile) to measure paw withdrawal latencies in response to radiant heat (55°C). A cutoff time of 20 s was used to prevent tissue damage in the absence of response. Mean paw withdrawal latencies were determined from the average of three separate trials, taken at 5 min intervals in each group of mice. The hot plate test was performed with a hot plate apparatus (Ugo Basile) at 52°C. We measured the time (in seconds) to paw licking or paw withdrawal in response to heat. For the

tail immersion test, about 3 cm of the distal part of the tail was immersed into a temperature-controlled water bath (52 ± 0.5°C). Latency was the time from tail immersion until it was removed or vigorously pulled away. The cutoff time was 20 s to prevent tissue damage.

Construction of Lenti-Drd1a-siRNAs. To silence dopamine D_1R expression *in vitro* and *in vivo*, three sequences were designed, targeted to different regions of the *Drd1a* mRNA sequence: (1) bp 82–89; (2) bp 1322–1329; (3) bp 720–729. These targets were selected based on Hannon's design criterion as indicated previously (Bahi et al., 2004a; Dreyer, 2010; Ramiro-Fuentes et al., 2010). An XhoI restriction site was added at the 3′ end of each oligo, and a U6–3′-specific 10mer was added at the 5′ end. Using the pSilencer 1.0-U6 (Ambion) as a template and a U6 promoter-specific forward primer containing the BamHI restriction site (GCGGATCCCGCTCTAGAACTAGTGC), each siRNA target was added to the mouse U6 promoter by PCR. Initial denaturation was 120 s at 94°C, followed by 35 cycles of the following program: 45 s at 94°C, 45 s at 64°C, and 45 s at 72°C. The PCR contained 4% dimethyl sulfoxide (Sigma). PCR products were digested with BamHI and XhoI, cloned into similar sites in pTK431, and sequenced to verify the integrity of each construct.

Lentivirus production. The vector plasmids pTK-Drd1a-siRNA and pTK433-GFP together with the packaging construct plasmid pΔNRF and the envelope plasmid pMDG-VSV-G were cotransfected into HEK293T cells to produce the viral particles, Lv-GFP or Lv-Drd1a-siRNA (Bahi et al., 2004a,b). Viral titers were determined by p24 antigen measurements (KPL). For *in vivo* experiments, viral stocks were matched for viral particle content and used at 2×10^9 particles/μl.

Determination of lentivirus silencing efficiency in vitro. The efficiency of the lentiviruses at silencing was tested *in vitro* in HEK293T cells. A total of 1×10^5 HEK293T cells were plated per well in six-well plates. The next day, lentivirus (Lv) stocks were mixed with 10 μg/ml Polybrene (Sigma), incubated for 30 min at room temperature, added to the cells, and incubated at 37°C. After 48 h, the medium was replaced with normal growth medium, and cells were left for an additional 48 h. Cells were then collected, and total RNA was isolated for real-time PCR. For *in vitro* silencing of *Drd1a*, cells were infected with 4 μl of Lv preparation, either 4 μl of Lenti-GFP used as control or 2 μl of Lenti-GFP plus 2 μl of one of the three Lenti-*Drd1a*-siRNA or plus 2 μl of all three Lenti-*Drd1a*-siRNAs together.

Quantitative real-time PCR. Primer sets for rat and mouse Drd1a, Drd2, and Gapdh were designed to amplify 100 to 200 bp products. The following specific primer pairs were used: Drd1a, 5′-AGGATTGCCCAGAAGCAAAT-3′ and 5′-GGGCACCATACAGTTCGAGA-3′; Drd2, 5′-CATTGTCTGGGTCCTGTTCCT-3′ and 5′-GACCAGCAGAGTGACGATGA-3′; Gapdh, 5′-ATGACTCTACCCACGGCAAG-3′ and 5′-CATACTCAGCACCAGCATCAC-3′. Gapdh was used as an endogenous control for normalization. Total RNA was extracted from the HEK293T cells (for *in vitro* quantification) or from the brains of treated animals (for *in vivo* quantification) using TRIzol reagent (Invitrogen) including an RNase-free DNase step. RNA was quantified by spectrophotometry, and its integrity was verified by agarose gel electrophoresis visualized with ethidium bromide. First-strand cDNA was generated from 2 μg of total RNA and Oligo ($dT_{12–18}$) primer with the Moloney murine leukemia virus reverse transcription kit (Invitrogen) in a total volume of 20 μl. Quantitative real-time PCR was performed in a real-time PCR iCycler (Bio-Rad). Five microliters of cDNA, 0.5 μM of forward and reverse primers, and 10 μl of IQ SYBR Green Supermix (Bio-Rad) were combined in a total volume of 20 μl. PCR was performed as follows: 3 min at 95°C (initial denaturation); 20°C/s temperature transition up to 95°C for 45 s, 45 s at 62°C, repeated for 40 cycles (amplification). The PCR was evaluated by melting-curve analysis and by checking the PCR products on a 2% agarose gel.

The PCR cycle number at which each assay target reached the threshold detection line was determined ("threshold cycles," Ct value). The Ct of each gene was normalized against that of *Gapdh* or *B-actin*. To determine the linearity and detection limit of the assay, successive 10-fold dilutions of each cDNA sample were amplified in a series of real-time PCRs, using duplicate assays for each dilution, so that the correlation coefficient could be calculated from the standard curve of Ct values. Comparisons were made between the different animal groups, and significance was calculated using two-tailed Student's *t* test. The level of statistical significance was set at $p < 0.05$. Data were expressed as mean ± SEM. The ΔCt for each candidate was calculated as ΔCt = [Ct (candidate) − Ct (*Gapdh* or *B-actin*)]. The relative abundance of each target in each protocol was calculated as the ratio between treated and untreated samples (Bahi and Dreyer, 2004; Bahi et al., 2004b; Mühlbauer et al., 2004).

Western blotting. The hippocampal region surrounding the siRNA injection site was dissected, homogenized in buffer (50 mM Tris, 300 mM NaCl, 1% Triton X-100, 25 mM NaF, 1 mM sodium orthovanadate, 4 mM sodium pyrophosphate, 1 mm EDTA, and 1 tablet of Complete protease inhibitor; Roche), and incubated at 4°C with shaking for 20 min. The samples were centrifuged at 10,000 × *g* at 4°C for 15 min. The protein concentration of the supernatants was quantified using the Bradford reaction. Equal amounts of total protein were subjected to SDS-PAGE, transferred to nitrocellulose membranes, and Western blotted following standard protocols. Membranes were blocked with 5% BSA in Tris-buffered saline–Tween 20, incubated with a primary antibody against D_1R (1:1000; Santa Cruz Biotechnology) overnight at 4°C, washed again, incubated for 1 h at room temperature with a peroxidase-conjugated secondary antibody, and visualized using ECL (GE Healthcare) and exposed to film for 1 min. Membranes were stripped, washed, and reprobed with glyceraldehyde-3-phosphate dehydrogenase (1:1000; Abcam). Exposed films were digitized and quantified with Quantity One software.

Surgery. As illustrated in Figure 7, we performed input–output curves, paired-pulse facilitation, and the LTP study in one set of four groups of animals: wild type, *Drd1a*$^{-/-}$, WT-GFP, and *Drd1a*-siRNA ($n = 10$ animals per group). We performed classical trace eyeblink conditioning in a separate set of animals including the same four genotypes/conditions (also $n = 10$ animals per group) (see Fig. 8).

Animals were anesthetized with 0.8–3% halothane (AstraZeneca). The gas mixture was delivered using a small anesthesia mask (David Kopf Instruments) connected to a calibrated Fluotec 5 (Fluotec-Ohmeda) vaporizer at a flow rate of 1–4 L/min oxygen. In the first surgical step, animals in groups WT-GFP and *Drd1a*-siRNA received a sterotaxic injection of 2 μl of Lv-GFP (WT-GFP) or a mix of Lv-*Drd1a*-siRNAs of concentrated lentiviral stocks (2×10^9 particles/μl) into the hippocampus. The injection was performed with a Hamilton syringe and performed unilaterally at the following coordinates, calculated from bregma and skull surface: anterior, −2.4; lateral, +1.5 (right side); ventral, −2.0 (Paxinos and Franklin, 2001).

As illustrated in Figure 1*A*, all animals included in the eight groups mentioned above were implanted with bipolar stimulating electrodes in the right Schaffer collateral–commissural pathway of the dorsal hippocampus (2 mm lateral and 1.5 mm posterior to bregma; depth from the brain surface, 1.0–1.5 mm) (Paxinos and Franklin, 2001) and with a recording electrode in the ipsilateral stratum radiatum underneath the CA1 area (1.2 mm lateral and 2.2 mm posterior to bregma; depth from the brain surface, 1.0–1.5 mm). These electrodes were made of 50 μm Teflon-coated tungsten wire (Advent Research Materials). The final position of hippocampal electrodes was determined as described previously (Gruart et al., 2006). The recording electrode was implanted in the CA1 area using as a guide the field potential depth profile evoked by paired (40 ms interval) pulses presented to the ipsilateral Schaffer collateral pathway. The recording electrode was fixed at the site where a reliable monosynaptic (≤5 ms) fEPSP was recorded.

Animals selected for the classical conditioning of eyelid responses were also implanted with stimulating electrodes on the left supraorbital nerve and with recording electrodes in the ipsilateral orbicularis oculi muscle (Fig. 1*A*). Electrodes were made of 50 μm Teflon-coated, annealed stainless steel wire (A-M Systems) bared at the tips for ~0.5 mm. The tips were bent into a hook to facilitate stable insertion in the upper eyelid.

A 0.1 mm bare silver wire was affixed to the skull as a ground. All the wires were connected to two four-pin sockets (RS-Amidata). The sockets were fixed to the skull with the help of two small screws and dental cement. The implantation procedures used in this chronic preparation have been described in detail (Gruart et al., 2006). Experimental sessions started 1 week after surgery. To verify the location of stimulating and recording electrodes after completion of experiments, mice were deeply reanesthetized (50 mg/kg sodium pentobarbital) and perfused/fixed

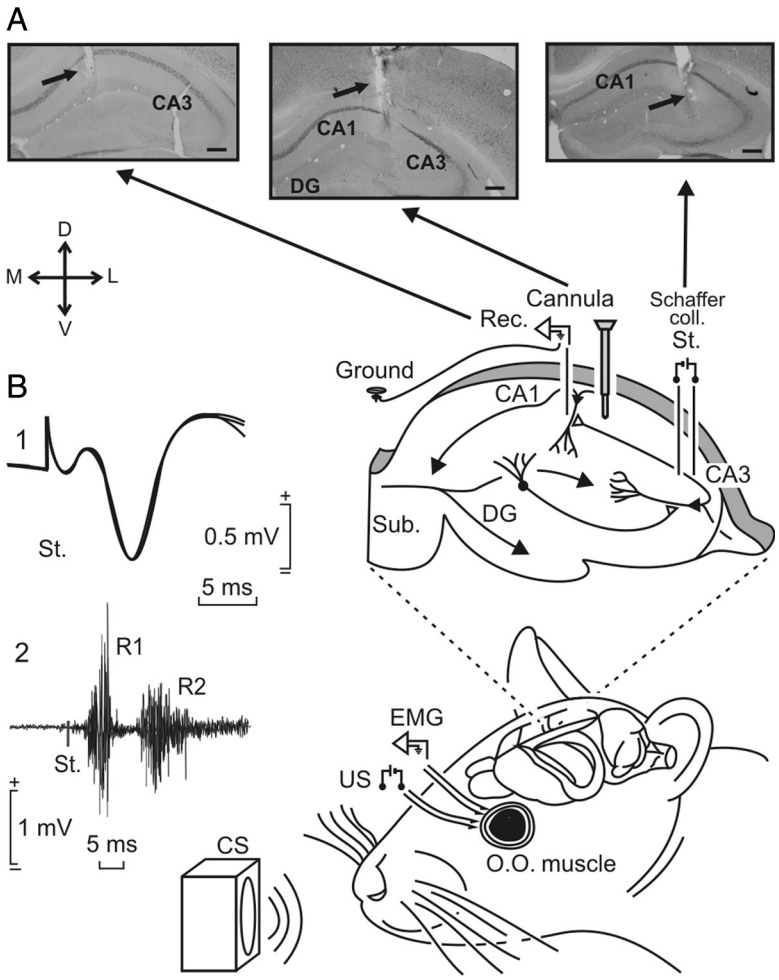

Figure 1. Experimental design for classical conditioning and LTP. Classical eyelid conditioning was achieved with a trace paradigm, using a tone as a CS. The loudspeaker was located 30 cm from the animal's head. Animals were implanted with bipolar stimulating electrodes on the left supraorbital nerve for US presentations. Eyelid conditioned responses were recorded with EMG electrodes implanted in the ipsilateral orbicularis oculi (O.O.) muscle. The top diagram illustrates that animals were also implanted with stimulating (St.) and recording (Rec.) electrodes to activate Schaffer collaterals and to record fEPSPs evoked at the pyramidal CA1 area of the right hippocampus and indicates the injection point for *Drd1a*-siRNA. ***A***, Photomicrographs illustrating the location of stimulating and recording electrodes and lentivirus injection site. Scale bars, 200 μm. DG, Dentate gyrus; Sub., subiculum; D, dorsal; L, lateral; M, medial; V, ventral. ***B***, The two sets of traces on the left illustrate the following: 1, a fEPSP evoked at the CA3–CA1 synapse; 2, an EMG recording evoked at the O.O. muscle by a single suprathreshold pulse presented to the supraorbital nerve. Both traces were collected during the ninth conditioning session of a control animal. Calibrations are as indicated.

transcardially with saline and 4% phosphate-buffered paraformaldehyde. Selected brain sections (50 μm thick) including the dorsal hippocampus were obtained in a microtome (Leica), mounted on gelatinized glass slides, and Nissl stained with 0.1% toluidine blue.

Electrophysiology. Recordings were made using six differential amplifiers with a bandwidth of 0.1 Hz to 10 kHz (P511; Grass-Telefactor) (Fig. 1*B*). Hippocampal recordings were made with a high-impedance probe (2×10^{12} Ω, 10 pF) (Fig. 1*B*).

For input–output curves, the stimulus intensity was raised to 0.3 mA in steps of 20 μA. The selected interstimulus interval was 40 ms, because it results in maximum facilitation of the CA3–CA1 synapse (Madroñal et al., 2007). For paired-pulse facilitation, pulse intensity (50–400 μA) was set at 30–40% of the amount necessary to evoke a maximum fEPSP response, and the following interstimulus intervals were used: 10, 20, 40, 100, 200, and 500 ms (Gureviciene et al., 2004). To avoid unwanted interactions between successive pairs of stimuli, the interpulse delay was always $\geq$20 s.

For evoking LTP, we used a high-frequency stimulation (HFS) train consisting of five 200 Hz, 100 ms trains of pulses at a rate of one per second. This protocol was presented six times, at intervals of 1 min. As indicated above for paired-pulse facilitation, pulse intensity was set at 30–40% of the amount necessary to evoke a maximum fEPSP response for baseline recordings and after the HFS train. To avoid evoking a population spike and/or unwanted EEG seizures, the stimulus intensity during the HFS train was set at the same intensity used for generating baseline records. Before presenting the animals with the HFS train, we collected baseline records for 15 min, by presenting single pulses (a 100 μs, square, negative–positive pulse) at a rate of one per 20 s. After the HFS train, we presented the same set of pulses for 30 min. An additional recording session lasting for 15 min was performed 24 h after the HFS session.

Classical eyeblink conditioning. For classical conditioning, using a trace paradigm, three animals at a time were placed in separate small ($5 \times 5 \times 10$ cm) plastic chambers located inside a larger ($30 \times 30 \times 20$ cm) Faraday box. Classical conditioning was achieved using a trace paradigm consisting of a tone (20 ms, 2.4 kHz, 85 dB) presented as a CS. The US consisted of a cathodal, square pulse applied to the supraorbital nerve (500 μs, three times the threshold) 500 ms after the end of the CS. A total of two habituation and 10 conditioning sessions were performed for each animal. A conditioning session consisted of 60 CS–US presentations and lasted ~30 min. For proper observation of conditioned response (CR) profiles, the CS was presented alone in 10% of the cases. CS–US presentations were separated at random by 30 $\pm$ 5 s. For habituation sessions, only the CS was presented, at the same frequency of 30 $\pm$ 5 s. Our criteria for CR were the presence, during the CS–US interval, of EMG activity lasting >10 ms and initiated > 50 ms after CS onset. In addition, the integrated EMG activity recorded during the CS–US interval had to be at least 2.5 times greater than the averaged activity recorded immediately before CS presentation (Porras-García et al., 2005). The total number of CRs per session was computed and expressed as a percentage of the maximum (60 CRs per session equal 100%).

Synaptic field potentials in the CA1 area were evoked during habituation and conditioning sessions by a single 100 μs square, biphasic (negative–positive) pulse applied to Schaffer collaterals 300 ms after CS presentation. Stimulus intensities ranged from 50 to 250 μA. For each animal, the stimulus intensity was selected according to data collected from the input–output curves, usually at ~30% of the intensity necessary for evoking a maximum fEPSP response (Gureviciene et al., 2004). An additional criterion for selecting stimulus intensity was that a second stimulus, presented 40 ms after a conditioning pulse, evoked a larger (>20%) synaptic field potential (Bliss and Gardner-Medwin, 1973).

Immnohistochemistry for Egr1. Mice used in the electrophysiology studies were fixed in 4% paraformaldehyde overnight, and brains were cut into 30 μm sections. Immunohistochemistry was done in free-floating sections with standard avidin–biotin immunocytochemical protocols (Rivera et al., 2002; Grande et al., 2004; Pavón et al., 2006; Granado et al., 2008) with specific polyclonal rabbit antisera raised against Egr1, formerly Zif268 (diluted 1:400; Santa Cruz Biotechnology). To enhance the staining, after incubation with the primary (one night) and secondary (2 h) antisera, sections were incubated for 1 h in a streptavidin–peroxidase complex (diluted 1:2000 in PBS-Triton X-100; Sigma). Peroxidase reactions were developed in 0.05% 3,3′-diaminobenzidine (Sigma) and

0.002% H_2O_2. Sections were then mounted on gelatin-coated slides, air dried, dehydrated in graded series of ethanol, cleared in xylene, and coverslipped with Permount mounting medium. Quantification of Egr1-positive nuclei in hippocampal sections was performed using an image analysis system (AIS; Imaging Research). Before counting, images were thresholded at a standardized gray-scale level, empirically determined by two different observers to allow detection of stained nuclei from low to high intensity, with suppression of the very lightly stained nuclei. The number of nuclei positive for Egr1 was determined and expressed as the number of positive nuclei per square millimeter (Granado et al., 2008). Counts were obtained from four hippocampal slices per animal (n = 10–12), for each group.

Statistical analysis. EMG and hippocampal activity, and 1 V rectangular pulses corresponding to CS and US presentations, were stored digitally on a computer through an analog/digital converter (1401 Plus; CED), at a sampling frequency of 11–22 kHz and an amplitude resolution of 12 bits. Commercial computer programs (Spike 2 and SIGAVG; CED) were modified to represent EMG and fEPSP recordings. Data were analyzed off-line for quantification of CRs and fEPSP slope using custom representation programs (Porras-García et al., 2005; Gruart et al., 2006). Computed data were processed for statistical analysis using the SPSS for Windows package. Unless otherwise indicated, data are represented as the mean ± SEM. Acquired data were analyzed using a two-way ANOVA, with group, session, or time as the repeated measure. Contrast analysis was added to further study significant differences. Regression analysis was used to study the relationship between the fEPSP slopes and the percentage of CRs.

Statistics on behavioral values to assess genotype and trial differences in the Barnes maze, active and passive avoidance, and the fear test were performed using repeated-measures, two-way ANOVA where genotype (wild type and *Drd1a*$^{-/-}$) and time (day of trials for passive avoidance or freezing test) were entered as independent variables. Relevant differences were analyzed pairwise by *post hoc* comparisons with Tukey's test. Immunohistochemical and Western blotting studies were analyzed using the Student's *t* test. For all statistical studies, SigmaStat 2.03 software was used, and the threshold for statistical significance was set at $p < 0.05$.

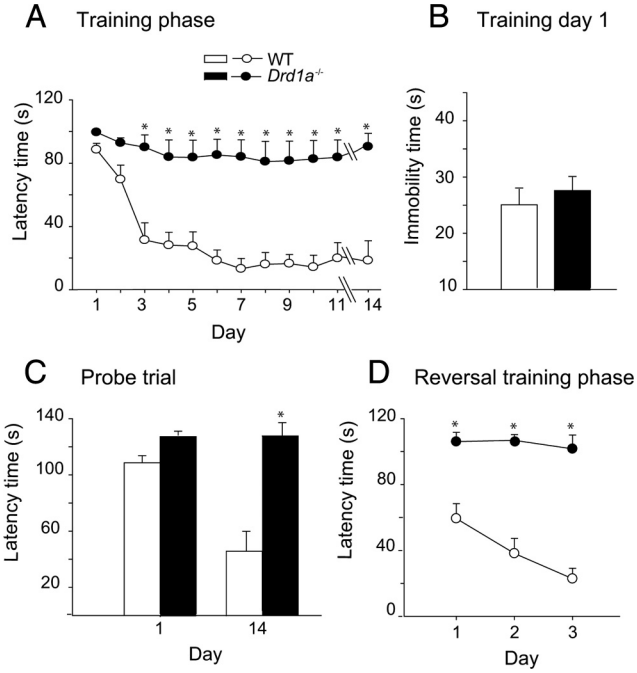

Figure 2. Hippocampus-dependent learning is impaired in dopamine *Drd1a*$^{-/-}$ mice. Data show the mean values ± SEM. ***A***, Progression of escape latency during the training phase in the Barnes maze. *Drd1a*$^{-/-}$ mice did not reduce escape latency at any time during the experiment (*$p < 0.005$). ***B***, Immobility during the first day of training. WT and *Drd1a*$^{-/-}$ mice showed similar levels of immobility. ***C***, Probe trial performed 3 d after the training phase. Histograms represent the time spent searching for the escape hole. *Drd1a*$^{-/-}$ mice did not reduce searching time during the probe trial (*$p < 0.005$). ***D***, Escape latency during the relearning phase. For this test, the escape hole was located opposite to its position in the training phase (*$p < 0.001$). Statistics were determined with repeated-measures two-way ANOVA followed by Tukey's test for *post hoc* analysis (***A***, ***D***) and with Student's *t* test (***C***).

Results

Barnes maze

To confirm the role of D_1R in spatial learning, we used the Barnes maze because it is less aversive and stressful than the water maze (Barnes, 1979; Harrison et al., 2009), and because previous studies have shown that the same mouse strain can perform differently in different spatial learning tasks (Patil et al., 2009; Zheng et al., 2009). In the Barnes maze, WT mice quickly learn to escape the open field and reach the black escape box, as shown by the rapid decline in escape latency (Fig. 2*A*). By day 7 of training, escape latency has reached a minimum that was maintained throughout the training phase (11 d) and during the probe trial, 3 d later. In contrast, there was no reduction in escape latency for the *Drd1a*$^{-/-}$ mice, even after an 11 d training period (Fig. 2*A*).

To rule out the possibility that inactivation of *Drd1a* increases anxiety levels in these mice, masking their capacity to respond in the Barnes maze, we evaluated the immobility time during the first day of training in the Barnes maze, as an indirect measure of anxiety. We chose the first day of training because on this day, the two groups showed similar latency times for crossing to the black escape box. WT and *Drd1a*$^{-/-}$ mice spend similar amounts of time immobile during the first day of training (Fig. 2*B*). Moreover, in the elevated-plus maze, which is commonly used as a direct test of anxiety, *Drd1a*$^{-/-}$ mice do not show higher anxiety levels than their WT littermates, as demonstrated by the number of entries and the time spent in the open arms (Fig. 3*A*).

In addition, *Drd1a*$^{-/-}$ mice showed no reduction in escape latency in a probe trial performed 3 d after training, to evaluate memory consolidation (Fig. 2*C*), or during the relearning trials, when the escape hole was moved to the opposite side of the training arena (Fig. 2*D*). With the previous study in the Morris maze (Granado et al., 2008), these data indicate that the D_1R is required for spatial learning in more than one paradigm. Our demonstration that loss of D_1R does not increase indicators of anxiety supports the notion that our results are attributable to an important role of D_1R in spatial learning.

Associative learning is impaired in *Drd1a*$^{-/-}$ mice

Active avoidance

Dopamine depletion impairs the acquisition and maintenance of conditioned avoidance responses (Shannon et al., 1999), suggesting that dopamine receptors are involved in this behavior. To determine whether the dopamine D_1R plays a role in this associative learning task, we used the two-way active avoidance paradigm. In this paradigm, WT mice learned the avoidance response within the first 2 d of training, while *Drd1a*$^{-/-}$ mice were unable to learn it, even with an extensive period of training (Fig. 4). Differences between the two groups were first evident on the second day of training ($p < 0.001$) and persisted throughout the experiment, demonstrating complete impairment of avoidance learning in *Drd1a*$^{-/-}$ mice (Fig. 4*A*).

The crossing latency reflects how rapidly the animal crosses to the safe compartment after the onset of the CS to avoid the footshock (Smith et al., 2002). WT animals progressively reduced their crossing latency, whereas *Drd1a*$^{-/-}$ mice did not, again indicating that *Drd1a*$^{-/-}$ mice were unable to learn that the footshock would follow the CS (Fig. 4*B*). Differences in latency be-

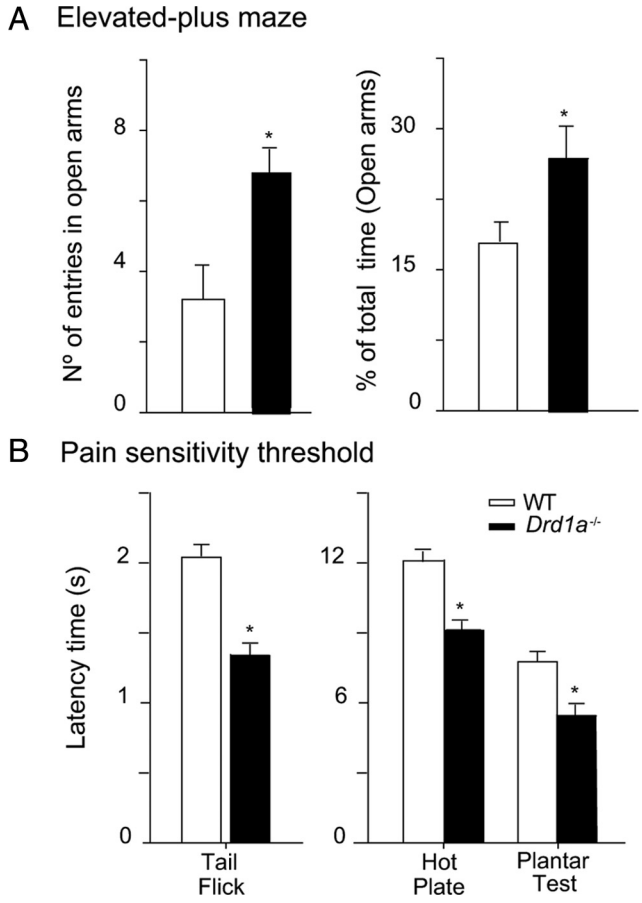

Figure 3. Anxiety levels are similar in both genotypes, but *Drd1a*$^{-/-}$ mice are more sensitive to pain than WT mice. ***A***, Anxiety-like behavior of *Drd1a*$^{-/-}$ and WT mice illustrated by the number of entries and percentage of total time (mean ± SEM) spent in the open arms of the elevated plus maze test. *Drd1a*$^{-/-}$ mice make more entries and spend more time in the open arms, indicating lower anxiety levels than the WT mice. *$p < 0.05$ versus WT mice. ***B***, Pain sensitivity thresholds (in seconds, mean ± SEM) of mice in tail flick, hot plate, and plantar tests. *Drd1a*$^{-/-}$ mice exhibit lower pain thresholds than WT mice in all three tests, indicating higher pain sensitivity. *$p < 0.05$ versus WT mice; $n = 8–10$ animals.

tween WT and *Drd1a*$^{-/-}$ mice were first observed on the second day of the training phase ($p < 0.001$).

Except for the first 2 d, we found no difference between wild type and *Drd1a*$^{-/-}$ in baseline crossing behavior, determined by counting crossings during the ITIs in the training phase or on the test day (Fig. 4*C*). Thus, the poor performance of the *Drd1a*$^{-/-}$ mice in this paradigm suggests impaired associative learning rather than changes in locomotor behavior.

Passive avoidance

Passive avoidance learning depends on multiple cortical and subcortical structures, including both dorsal and ventral striatum as well as hippocampus and amygdala (Pittenger et al., 2006). In this test, avoidance response or entry latency increases with footshock intensity (Crawley, 2007). First, we determined the sensitivity to footshock for both genotypes by gradually increasing footshock intensity (0.01–0.6 mA) and monitoring the onset of behavioral indicators of sensation or pain. Wild type and *Drd1a*$^{-/-}$ showed similar sensitivity thresholds to footshock (Fig. 5*A*), responding with a sudden stare at floor bars, startle response, and jumping and vocalization at the same footshock intensities in both genotypes. Jumping and vocalization responses, indicative of pain threshold, were elicited with 0.12 mA in both groups of mice. Passive avoidance experiments were performed with a moderate (0.4 mA) and a strong (0.8 mA) electric stimulus (Viosca et al., 2009), both well above the pain threshold (Fig. 5*A*). Baseline entry latency times in the passive avoidance test were similar in all experimental groups. However, after training with either 0.4 or 0.8 mA footshock, *Drd1a*$^{-/-}$ mice exhibited a shorter latency than WT mice (Fig. 5*B*), indicative of reduced memory strength. When animals were tested 24 h after 0.4 mA footshock, WT mice showed a latency time of 250 s compared with 123 s in *Drd1a*$^{-/-}$ mice ($p < 0.001$). With an 0.8 mA shock, this difference was smaller but still statistically significant ($p < 0.05$) (Fig. 5*B*). To exclude the possibility that *Drd1a*$^{-/-}$ are simply less sensitive to electric shock/pain than WT animals, we determined pain thresholds for both genotypes using tail flick, hot plate, and plantar tests. In all three assays, the pain threshold was actually lower for *Drd1a*$^{-/-}$ than WT mice (Fig. *3B*), indicating that *Drd1a*$^{-/-}$ mice are actually more sensitive to footshock than WT mice and supporting the conclusion that our results in the passive avoidance test reflect an important role of *Drd1a*$^{-/-}$ in this type of associative learning.

Fear conditioning learning

We studied the role of dopamine D_1Rs in fear memory using both contextual fear conditioning, which is dependent on both the hippocampus and the amygdala, and cued fear conditioning, which is dependent only on the amygdala. Our protocol allowed us to test both contextual and cued fear conditioning in one experiment. Baseline levels of freezing were equal in wild type and *Drd1a*$^{-/-}$ during training, as were levels of freezing after footshock. Then, 24 h after training, animals were reexposed to the training context. As expected, freezing levels in WT mice were significantly elevated to 60% of the total time. Although freezing was also elevated in *Drd1a*$^{-/-}$ mice, it was much lower than in WT mice. *Drd1a*$^{-/-}$ mice spent only 22% of the time freezing (Fig. 5*C*). When animals were exposed to a new context, both genotypes decreased their freezing levels compared with context testing levels, but freezing levels in WT mice remained significantly higher than in *Drd1a*$^{-/-}$. When the CS (tone) was presented in the new context, both genotypes increased their freezing levels significantly, but again, WT mice spent significantly more time freezing than *Drd1a*$^{-/-}$ (Fig. 5*C*). Altogether, these results indicate that the D_1R is necessary for cued and contextual associative learning.

To study extinction, we wanted to start with equal freezing times in the two genotypes because 24 h after a single footshock, freezing times were significantly different in wild type and *Drd1a*$^{-/-}$. Therefore, 48 h after the first footshock, we delivered three consecutive footshocks separated by 30 s, which resulted in equal freezing times in both genotypes. After this, mice were tested daily in the same context for 6 consecutive days, revealing similar extinction curves for both genotypes: by 1 week after the footshocks, both groups of mice had reduced freezing time by 50% (data not shown). These results suggest that D_1R is not necessary for extinction.

In vitro and *in vivo* siRNA-mediated knockdown of dopamine D_1R

To rule out developmental effects of the absence of the D_1R in *Drd1a*$^{-/-}$ mice, we used Lv-based RNA interference to knock down dopamine D_1R expression in adult animals. We designed three siRNAs targeted against different regions of the *Drd1a* mRNA. These were inserted into the transfer plasmid of the Lv system, and their efficiency at silencing *Drd1a* was assessed in HEK293T cells (Fig. 6*A*). Then, 4 d after infection, *Drd1a* transcripts were measured by quantitative reverse transcription (RT)-

PCR. Infection with Lv-*Drd1a*-siRNA 1, 2, or 3 individually resulted in dopamine *Drd1a* downregulation, yielding residual *Drd1a*$^{-/-}$ expression levels of 40, 15, and 60%, respectively. However, coinfection with all three Lv-*Drd1a*-siRNAs decreased *Drd1a* mRNA expression by >93% (Fig. 6*A*). Control infection with Lv-GFP did not alter *Drd1a* expression in these cells (Fig. 6*A*).

To assess whether Lv-*Drd1a*-siRNAs can deplete D_1R expression *in vivo*, the nucleus accumbens (NAc) and the hippocampus were injected stereotaxically with the mix of Lv-*Drd1a*-siRNAs (2 μl) or with Lv-GFP as a control. Two weeks after the injection, there were dramatic decreases in D_1R protein or gene (*Drd1a*$^{-/-}$) expression in these regions in *Drd1a*-siRNA-injected mice compared with animals given injections of Lv-GFP (WT-GFP). We include the NAc in this experiment because the expression of D_1R in this nucleus is higher than that in the hippocampus, and this allows us to better assess the capacity of our vectors to silence D_1R. Quantitative RT-PCR revealed an 80% decrease in *Drd1a* mRNA expression in the NAc (Fig. 6*B*), and Western blotting revealed a 73% decline in D_1R protein in the hippocampus (Fig. 6*C*). Both decreases were statistically significant compared to WT-GFP. *Drd2* receptor mRNA expression was not affected, indicating that the *Drd1a* siRNA mix was highly specific for dopamine D_1R (Fig. 6*B*). We determined the spread of the virus within the hippocampus in the WT-GFP-injected mice using immunohistochemistry and found that particles infected ~2 mm^2 along the rostrocaudal axis, infecting most of the dorsal hippocampus, including the pyramidal cell layer and dentate gyrus (Fig. 6*D*,*E*).

In vivo basal synaptic transmission is normal in *Drd1a*$^{-/-}$ and in *Drd1a*-siRNA mice

We measured fEPSPs evoked at the CA3–CA1 synapse by *in vivo* electrical stimulation of Schaffer collaterals in the following groups of mice: wild type, *Drd1a*$^{-/-}$, wild type injected with Lv-*Drd1a*$^{-/-}$-siRNA (*Drd1a*-siRNA), and WT-GFP. Input–output curves using a wide range of stimulus intensities (0.02–0.4 mA) and paired (S1, S2) pulses at a fixed interval of 40 ms revealed no significant differences in basal synaptic transmission between the four groups (Fig. 7*A*,*B*). Interestingly, the combined value of fEPSPs evoked by both stimuli (S1 plus S2) presented an exponential relationship ($r \leq 0.98$; $p < 0.0001$) with stimulus intensity, with no significant differences ($p \geq 0.1925$) between the four groups. The stimulus intensities used in the remainder of this study were selected from within a range of 30–40% of the saturating intensity, intensities able to evoke facilitation of the second pulse.

Paired-pulse facilitation *in vivo* is normal in *Drd1a*$^{-/-}$ and in *Drd1a*-siRNA mice

Using the double-pulse test with interpulse intervals ranging from 10 to 500 ms, we found a significant ($p < 0.001$) increase in slope of fEPSPs evoked by the second pulse at short time intervals (20, 40, and 100 ms). There were no significant differences be-

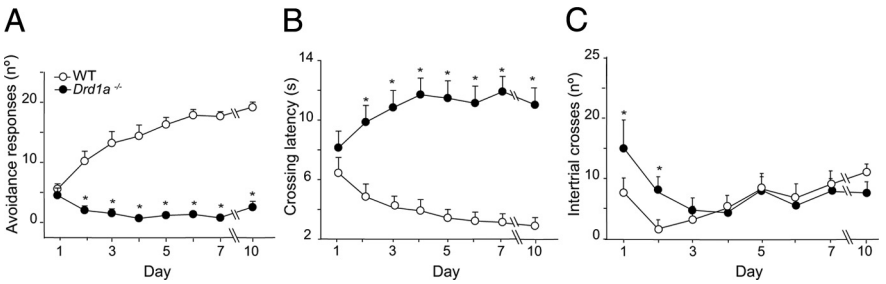

Figure 4. Active avoidance performance is impaired in dopamine *Drd1a*$^{-/-}$ mice. Data shown are mean values ± SEM. ***A***, Progression of active avoidance responses during the training phase. *Drd1a*$^{-/-}$ mice did not increase the number of avoidance responses during the training phase (*$p < 0.001$.). ***B***, Time course of crossing latencies for WT and *Drd1a*$^{-/-}$ mice during the training phase. *Drd1a*$^{-/-}$ mice did not decrease escape latency at any point during training (*$p < 0.001$). ***C***, Number of intertrial crosses. From day 3 on, there was no significant difference between WT and *Drd1a*$^{-/-}$ mice in the number of intertrial crosses. Statistics were performed with repeated-measures two-way ANOVA, followed by *post hoc* analysis with Tukey's test.

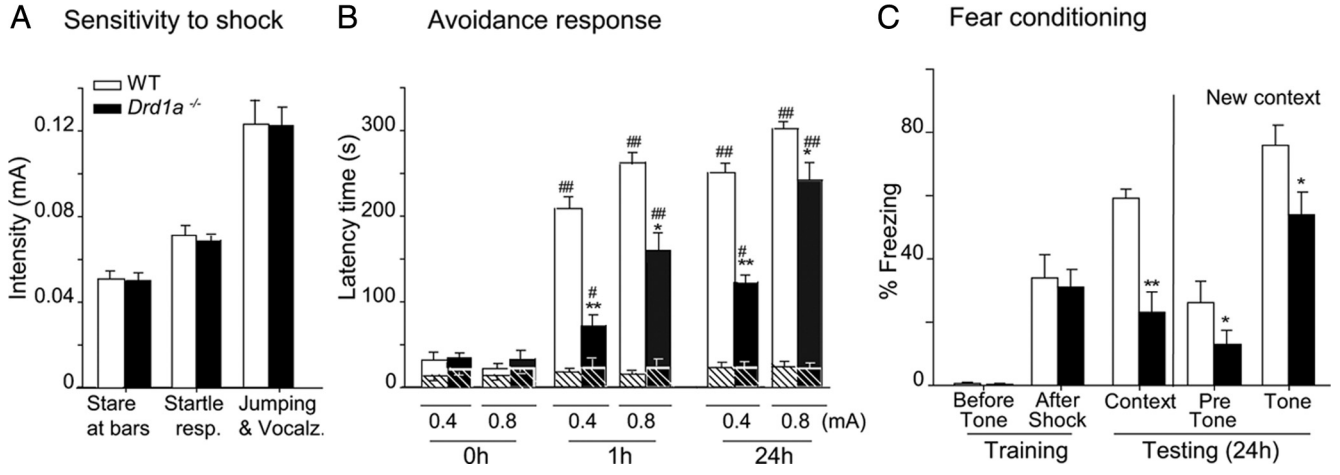

Figure 5. Performance in the passive avoidance test and fear conditioning are impaired in *Drd1a*$^{-/-}$ mice. Data show mean ± SEM. ***A***, Thresholds for footshock responses. Increasing intensity footshocks were delivered to WT and *Drd1a*$^{-/-}$ mice, and the threshold for each listed behavior was determined. Thresholds for all three response behaviors were similar in the two genotypes. ***B***, Avoidance response. Latency refers to the time spent in the light compartment before mice enter the dark compartment, which was paired with footshock in a single training trial. *Drd1a*$^{-/-}$ mice show partial impairment of passive avoidance at both 0.4 and 0.8 mA. ***C***, Cued and contextual fear conditioning are impaired in *Drd1a*$^{-/-}$ mice. Freezing time was measured in contextual and cued fear conditioning trials 24 h after training. *$p < 0.01$ and **$p < 0.001$ versus wild type; #$p < 0.01$ and ##$p < 0.001$ versus Pre-shock (0 h). Statistics were determined by repeated-measures two-way ANOVA followed by *post hoc* analysis with Tukey's test.

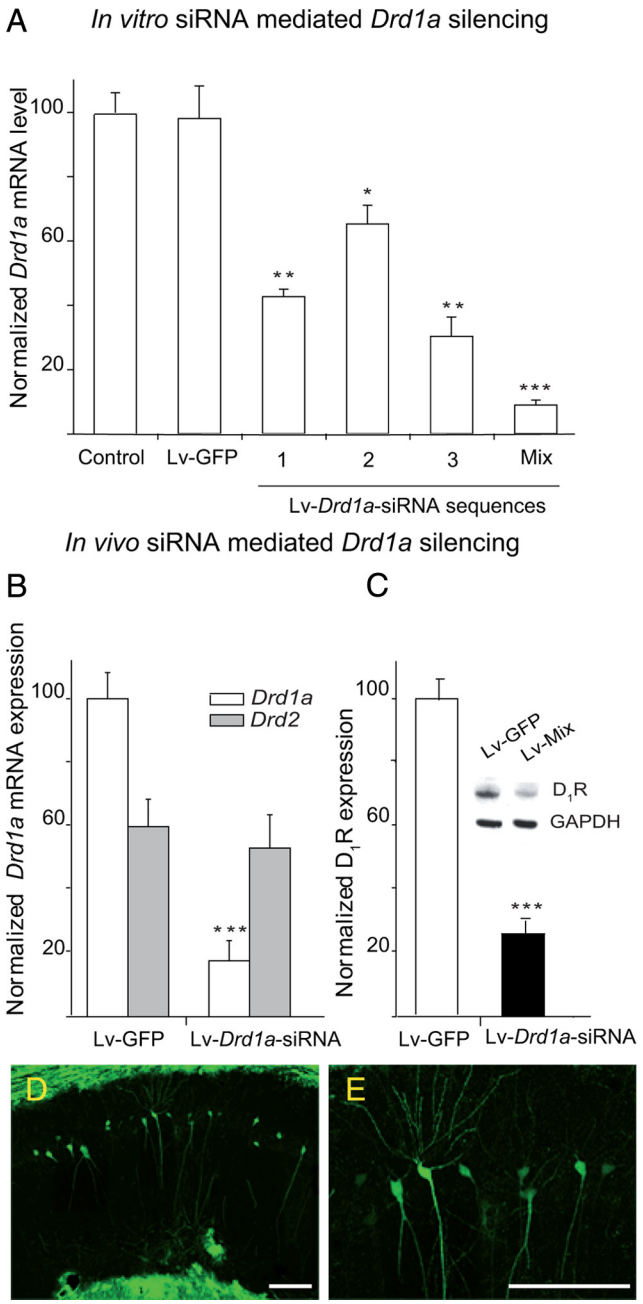

Figure 6. siRNA-mediated *Drd1a* silencing *in vitro* and *in vivo*. ***A***, Drastic reduction of *Drd1a* mRNA expression in HEK cells *in vitro* after infection with *Drd1a*-siRNA constructs. mRNA levels were determined by quantitative RT-PCR 48 h after infection and normalized to *Gapdh* mRNA levels. $*p < 0.05$; $**p < 0.01$; $***p < 0.005$; one-way ANOVA. ***B***, *Drd1a* and *Drd2* mRNA levels in NAc 48 h after intra-accumbal injection of a mixture of all three *Drd1a*-siRNAs. mRNA levels were determined by RT-PCR, normalized to *Gapdh*, and expressed as a percentage of *Drd1a* mRNA expression in Lv-GFP-injected animals. Injection of *Drd1a*-siRNAs specifically decreased *Drd1a* mRNA expression. ***C***, D_1R protein expression in hippocampus 48 h after injection of *Drd1a*-siRNAs. D_1R protein levels were decreased ~75%. $***p < 0.001$, Student's *t* test. ***D***, Photomicrograph of a coronal brain section illustrating the spread of lentiviral infection in the CA1 layer of the hippocampus of WT mice injected with 2 μl of Lenti-GFP particles. ***E***, High-magnification image of infected pyramidal cells illustrated in ***D***. Particles infect most of the dorsal hippocampus spreading through pyramidal CA1 cell layer. Scale bar, 100 μm.

tween WT, *Drd1a*$^{-/-}$, WT-GFP, and *Drd1a*-siRNA mice ($p = 0.959$) (Fig. 7*C*). These results are similar to those obtained in *Drd1a*$^{-/-}$ *in vitro* (Granado et al., 2008) and confirm that D_1Rs are not involved in this form of very short-term plasticity.

Hippocampal LTP *in vivo* is significantly reduced in *Drd1a*$^{-/-}$ and in *Drd1a*-siRNA mice

To explore the role of the D_1R in hippocampal LTP, we compared CA3–CA1 fEPSPs after HFS of Schaffer collaterals in WT, *Drd1a*$^{-/-}$, WT-GFP, and *Drd1a*-siRNA mice (Fig. 7*D*,*E*). To determine baseline responses, Schaffer collaterals were stimulated every 20 s for 15 min. The stimulus consisted of a 100 μs square, negative–positive pulse. After HFS, the same single stimulus was presented every 20 s for 30 min and repeated 24 h later, for 15 min. We found significant LTP in WT and WT-GFP mice. As expected, 15 min after HFS, the response to the single stimulus in both WT and WT-GFP groups was >200% of baseline values ($p < 0.001$) (Fig. 7*D*,*E*, open circles). Significant LTP persisted at 24 h post-HFS ($p < 0.001$) (Fig. 7*D*,*E*). In contrast, *Drd1a*$^{-/-}$ showed no LTP at the CA3–CA1 synapse after HFS. Indeed, 15–30 min after HFS, fEPSP slopes in *Drd1a*$^{-/-}$ mice were not significantly different (~140%; $p = 0.138$) from baseline (Fig. 7*D*, filled circles). In *Drd1a*-siRNA mice, the fEPSP slope was not significantly different from baseline at any time after HFS ($p = 0.146$) (Fig. 7*E*, filled squares). These data suggest that D_1R plays a crucial role in induction of LTP at the CA3–CA1 synapse after HFS of Schaffer collaterals *in vivo*.

Classical trace eyeblink conditioning is significantly reduced in *Drd1a*$^{-/-}$ and *Drd1a*-siRNA mice

First, we verified that the neural premotor circuits involved in the generation of eyelid responses function normally in the four groups of animals used in this study (wild type, *Drd1a*$^{-/-}$, WT-GFP, and *Drd1a*-siRNA). As illustrated in Figure 1*B*2, the blink reflex is easily characterized by measuring the latency of its early (R1) and late (R2) components (Kugelberg, 1952) and the corresponding integrated EMG areas (Gruart et al., 1995). Eyeblinks evoked by electrical stimulation of the ipsilateral supraorbital nerve in the WT group presented values (R1 latency, 4.9 ± 1.3 ms; R2 latency, 11.2 ± 3.3 ms; R1+R2 integrated area, 79.2 ± 15.6 μV × s) in the range of previous descriptions in mice (Gruart et al., 2006). There were no significant differences between our four groups of mice in the baseline blink reflex ($p \leq 0.713$).

To investigate the possible behavioral consequences of the deficit in synaptic plasticity at the CA3–CA1 synapse observed in *Drd1a*$^{-/-}$ and *Drd1a*-siRNA mice, we evaluated classical conditioning of eyeblink responses in the four groups of experimental animals using a trace paradigm (CS, tone; US, shock) with a 500 ms interval between the end of the CS and the beginning of the US (Fig. 8*A*,*B*). In WT mice, the percentage of CRs increased significantly across conditioning sessions ($p < 0.001$) (Fig. 8*C*), with a profile similar to that reported previously (Takatsuki et al., 2003; Gruart et al., 2006). In contrast, the percentage of CRs in the *Drd1a*$^{-/-}$ group was not significantly different from habituation values ($p = 0.431$) at any point over the course of conditioning. The percentage of CRs presented by the WT group was significantly different from that of the *Drd1a*$^{-/-}$ group from the 4th to the 10th conditioning session ($p < 0.001$) (Fig. 8*C*). Similarly, WT-GFP animals presented learning curves similar to those seen in WT mice, whereas CRs in *Drd1a*-siRNA mice were not significantly above baseline ($p < 0.001$) (Fig. 8*D*).

Evolution of CA3–CA1 fEPSP across classical conditioning: inactivation of D_1R impairs CA3–CA1 synaptic efficiency induced during classical conditioning

As shown recently in behaving mice, trace eyeblink conditioning is associated with increases in synaptic efficiency at CA3–CA1 synapses (Gruart et al., 2006). We therefore evaluated the effect of

D_1R loss on CA3–CA1 fEPSPs. Electrical stimulation of Schaffer collaterals 300 ms after CS presentation evoked a fEPSP in the CA1 area in all four experimental groups (Fig. 8*A*,*B*). Although the stimuli presented to Schaffer collaterals disrupted the regular theta rhythm recorded in the CA1 area, the rhythm reappeared in phase ~200 ms afterward. The slope of the evoked fEPSPs increased in the four experimental groups over the course of conditioning (Fig. 8*E*,*F*). These increases in fEPSP slopes across conditioning sessions were only observed for recordings collected during the CS–US interval with the animal placed in the recording box (i.e., fEPSPs were not modified by the mere repetitive stimulation of Schaffer collaterals).

There were clear differences between the two control (WT and WT-GFP) groups and the two experimental (*Drd1a*$^{-/-}$ and *Drd1a*-siRNA) groups. By the fourth conditioning session, fEPSP slopes recorded in WT (143%) and WT-GFP (134%) mice were significantly elevated over baseline values ($p < 0.001$) (Fig. 8*E*,*F*), consistent with previous studies (Gruart et al., 2006). In contrast, from the fourth conditioning session on, although the slopes of evoked fEPSPs in *Drd1a*$^{-/-}$ (114%) and *Drd1a*-siRNA (116%) mice were slightly (although nonsignificantly) elevated over baseline, they were significantly smaller than in corresponding control animals (Fig. 8*E*,*F*). Thus, the decreased performance in associative learning tasks seen in *Drd1a*$^{-/-}$ and *Drd1a*-siRNA mice compared with their respective controls is paralleled by a dramatic decline in activity-dependent increases in synaptic efficiency at the CA3–CA1 synapse during classical conditioning.

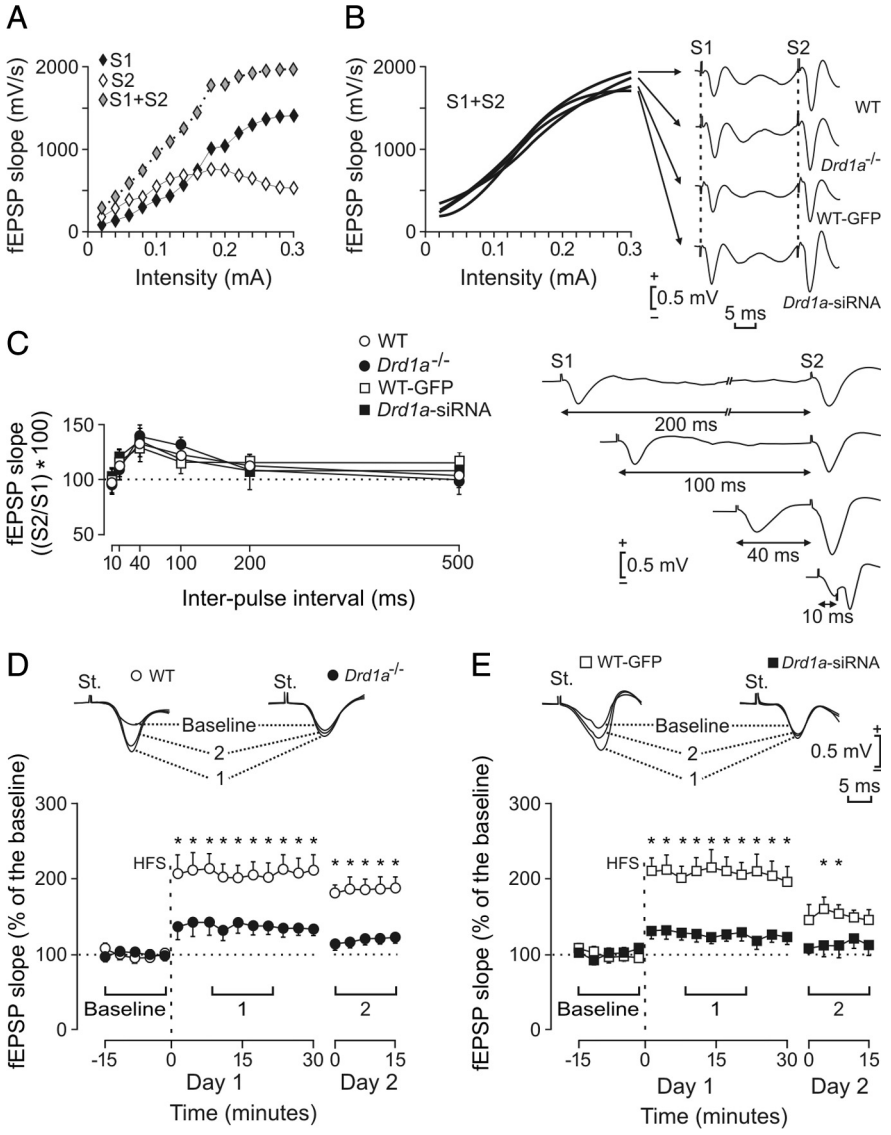

Figure 7. Input–output curves, paired-pulse facilitation, and LTP induction in the CA1 area in wild type, *Drd1a*$^{-/-}$, WT-GFP, and *Drd1a*-siRNA. ***A***, Representative example of an input–output curve collected from a *Drd1a*$^{-/-}$ mouse. Stimulus consisted of paired (S1, S2) pulses (40 ms interpulse interval) presented at increasing intensities in 20 μA steps. Note the sigmoid shape of S1 + S2 value. ***B***, The four experimental groups presented similar sigmoid curves for S1 + S2 values ($n = 10$ animals per group). Representative sample records collected from the four experimental groups are illustrated on the right. ***C***, Paired-pulse facilitation of fEPSPs recorded in the CA1 area after stimulation of Schaffer collaterals. The data shown are mean ± SEM. slopes of the second fEPSP expressed as a percentage of the first for the six interpulse intervals. No significant differences were observed between the four experimental groups. Extracellular fEPSP paired traces were collected from a representative *Drd1a*-siRNA animal at the indicated interstimulus intervals. ***D***, Top, Representative fEPSPs recorded from WT and *Drd1a*$^{-/-}$ animals before (baseline), and 15–30 min (1) and 24 h (2) after HFS. Graphs illustrate the time course of changes in fEPSPs (mean ± SEM) after HFS stimulation of the Schaffer collaterals. The HFS train was presented after 15 min of baseline recordings, at the time indicated by the dashed line. fEPSP slopes are expressed as a percentage of the baseline (100%) slope. WT mice exhibited significantly greater LTP than *Drd1a*$^{-/-}$ mice (*$p < 0.001$). ***E***, Same analysis as in ***D*** for WT-GFP and *Drd1a*-siRNA groups. Here again, the control group (WT-GFP) presented significantly larger LTP than *Drd1a*-siRNA mice (*$p < 0.01$). St., Stimulating electrode.

In vivo HFS-induced expression of Egr1 in the hippocampus is reduced in *Drd1a*$^{-/-}$ and *Drd1a*-siRNA mice

Hippocampal *Egr1/zif268* expression is required for late LTP and memory formation (Guzowski et al., 2000; Hall et al., 2001; Jones et al., 2001; Kelly and Deadwyler, 2003; McIntyre et al., 2005; Granado et al., 2008). Our results reveal that the D_1R is required for CA3–CA1 LTP induced by HFS of the Schaffer collaterals, as well as for classical eyeblink conditioning and the associated increase in CA3–CA1 synaptic efficiency. To explore whether *Egr1* induction by HFS *in vivo* requires dopamine D_1R, we examined Egr1 protein expression in the hippocampus of WT, *Drd1a*$^{-/-}$, *Drd1a*-siRNA, and WT-GFP mice after HFS of the Schaffer collaterals. Basal expression of Egr1 in the hippocampus was similar in all groups (Fig. 9*A*–*D*, Table 1), with a moderate number of neurons expressing Egr1 constitutively. Then, 24 h after *in vivo* tetanic stimulation of the CA3 cell layer, Egr1 expression increased significantly in the hippocampus of WT and WT-GFP animals (Fig. 9, *E* and *G*, respectively) compared with nonstimulated animals (Fig. 9*A*,*C*). Staining was particularly intense in cells along the dorsal CA1 region. Genetic inactivation or siRNA silencing of *Drd1a* significantly inhibited induction of Egr1 expression after *in vivo* tetanic stimulation (Fig. 9*F* and *H*, respectively). Quantification revealed that HFS-induced Egr1 expression decreased by

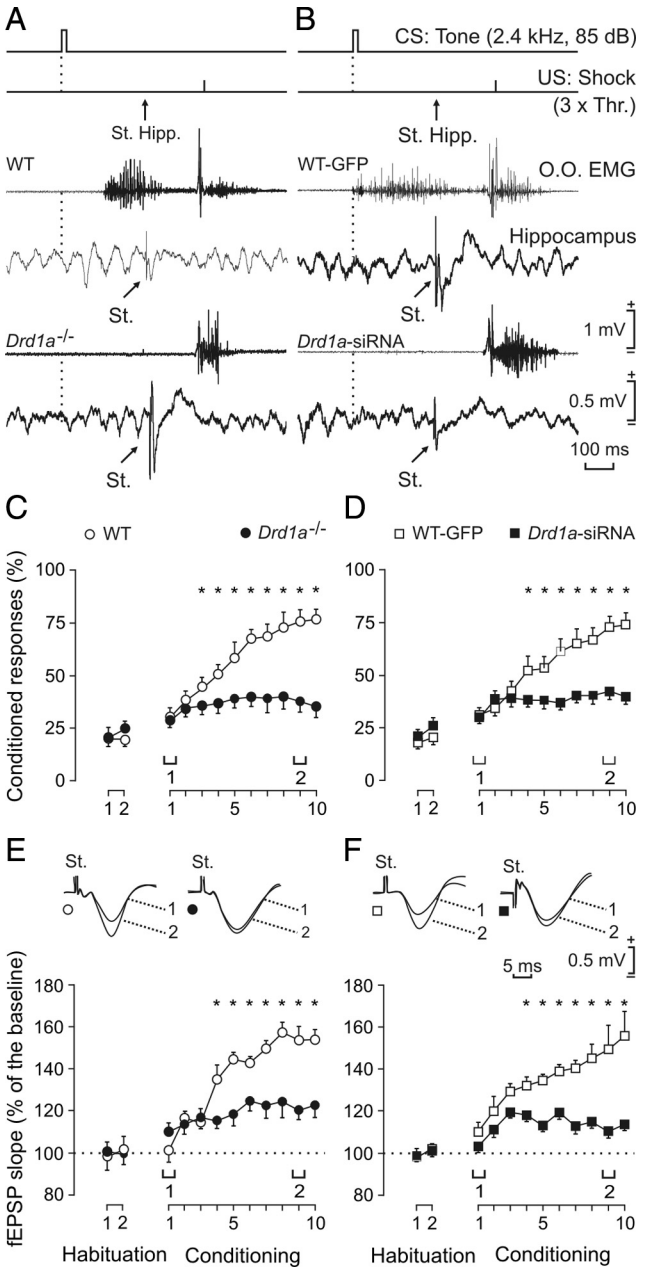

Figure 8. Evolution of CA3–CA1 synaptic field potentials and learning curves for WT, *Drd1a*$^{-/-}$, WT-GFP, and *Drd1a*-siRNA. ***A***, ***B***, Top to bottom, the conditioning paradigm, representative EMG, and representative hippocampal recordings during paired CS–US presentations for WT and *Drd1a*$^{-/-}$ mice (***A***) and for WT-GFP and *Drd1a*-siRNA mice (***B***). The time of stimulus presentation at Schaffer collaterals (St. Hipp.) is indicated, as are the times of delivery of CS (dashed line) and US. Data shown were collected during the ninth conditioning session. 3× Thr., Three times threshold. ***C***, ***D***, Percentage of eyelid CRs reached by the four experimental groups. The acquisition curve presented by the WT group (open circles) was significantly larger than values reached by the *Drd1a*$^{-/-}$ group (***C***, filled circles; $*p < 0.001$). Similarly, the acquisition curve of the WT-GFP group was also significantly larger than that presented by *Drd1a*-siRNA animals (***D***; $*p < 0.001$). ***E***, ***F***, Evolution of fEPSPs evoked at the CA3–CA1 synapse across conditioning for WT and *Drd1a*$^{-/-}$ mice (***E***) and for WT-GFP and *Drd1a*-siRNA animals (***F***). fEPSP slope is expressed as a percentage of fEPSP slope during habituation for each group. Differences in fEPSP slopes between WT and *Drd1a*$^{-/-}$ groups were statistically significant from the 4th to the 10th conditioning sessions (***E***; $*p < 0.006$), as well as between WT-GFP and *Drd1a*-siRNA animals (***F***; $*p < 0.001$), indicating that activity-dependent synaptic plasticity was severely impaired in both *Drd1a*$^{-/-}$ and *Drd1a*-siRNA mice. St., Stimulating electrode.

~50% in *Drd1a*$^{-/-}$ mice and by 60% in *Drd1a*-siRNA mice (Table 1). These results indicate that expression of D_1R is important for induction of Egr1 by tetanization *in vivo* in the rodent hippocampus.

Discussion

Our principal finding is that associative learning is abolished or dramatically reduced in *Drd1a*$^{-/-}$ mice and mice given intrahippocampal injections of Lv-*Drd1a*-siRNA. In addition, both LTP induced at the CA3–CA1 synapse by *in vivo* HFS of the Schaffer collaterals and the physiological potentiation that occurs at CA3–CA1 synapses in parallel with acquisition of classical conditioning of eyelid responses are significantly impaired in *Drd1a*$^{-/-}$ and *Drd1a*-siRNA mice. These data extend our previous finding that the D_1R is necessary for evoking early and late LTP *in vitro* (Granado et al., 2008). More importantly, our finding that acquisition of associative learning and the physiological increase in synaptic strength at the CA3–CA1 synapse in alert behaving mice are drastically reduced in D_1R-depleted mice provides evidence for a functional relationship between associative learning and synaptic plasticity in this region.

It has been suggested that the Barnes maze discriminates spatial learning more clearly than the Morris water maze (Barnes, 1979; Harrison et al., 2009; Patil et al., 2009; Zheng et al., 2009) and is useful when the Morris water maze shows partial impairment. *Drd1a*$^{-/-}$ mice were tested in the Barnes maze to consolidate the finding that D_1R is necessary for spatial learning in the Morris maze. Our results are in agreement with previous results from our laboratory (Granado et al., 2008) and others (Smith et al., 1998). Unlike a previous water maze study in which *Drd1a*$^{-/-}$ mice did learn after extended training (El-Ghundi et al., 1999), we saw no decrease in the escape latency for *Drd1a*$^{-/-}$ mice in the Barnes maze, even after extended training. Two indicators of anxiety level, immobility during the first day of training in the Barnes maze and performance in the elevated plus maze, revealed no increase in anxiety in the knock-out animals, so it is unlikely that the impaired performance of *Drd1a*$^{-/-}$ mice in the Barnes maze is attributable to an effect of the knockout on anxiety. Our results confirm the crucial role of D_1R in spatial learning.

While spatial memory is hippocampus-dependent, other forms of associative learning also depend on the amygdala. To further assess the role of D_1R in associative learning, we used three paradigms that evaluate fear memory. In the active avoidance test, *Drd1a*$^{-/-}$ mice did not decrease their escape latency at any point during the training trials. Similar random crossing scores for WT and *Drd1a*$^{-/-}$ mice indicate that this finding is not caused by decreased locomotor activity. The results of our passive avoidance trials also confirm that this learning impairment was not caused by locomotor deficits or freezing. In passive avoidance, *Drd1a*$^{-/-}$ showed some learning at 0.4 or 0.8 mA but were significantly impaired compared with WT mice 1 and 24 h after training. Sensitivity to footshock was similar in WT and *Drd1a*$^{-/-}$, so altered sensitivity or pain threshold was not a factor. Thus, the avoidance impairment associated with D_1R inactivation is likely attributable to abnormal acquisition of learning or to abnormal short-term memory retrieval, but not to deficits in memory consolidation. These mice showed similar avoidance responses at 1 and 24 h after the shock, indicating that they are able to retrieve what they have learned.

We used the fear conditioning test to discriminate between hippocampus- and amygdala-dependent associative learning. *Drd1a*$^{-/-}$ animals were impaired in both contextual (hippocampus-dependent) and cued (hippocampus- and

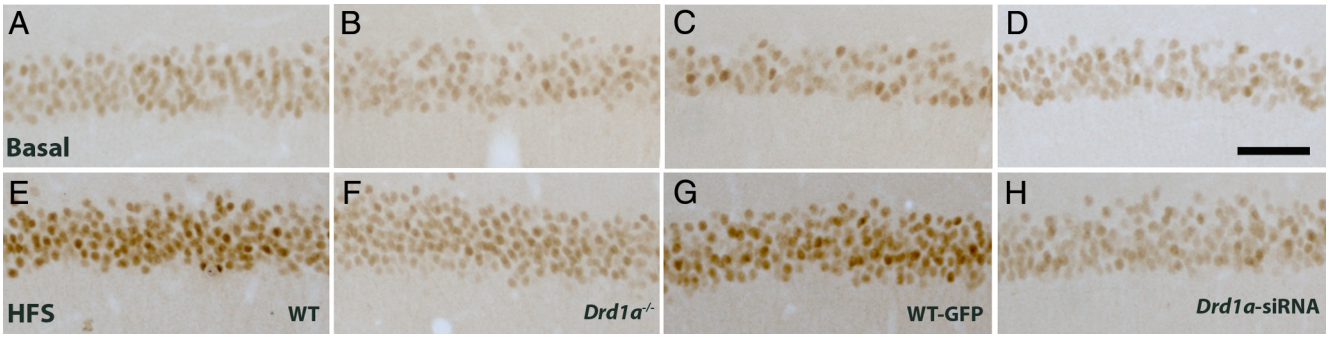

Figure 9. D_1R is required for activity-induced Egr1 in CA1 pyramidal cells after HFS of Schaffer collaterals. Photomicrographs of the CA1 pyramidal cell layer of the hippocampus from coronal brain slices showing immunohistochemistry for the Egr1 transcription factor are presented. ***A–D***, Egr1 expression under basal conditions for WT, *Drd1a*$^{-/-}$, WT-GFP, and *Drd1a*-siRNA mice, respectively. ***E–H***, Expression 24 h after *in vivo* HFS of the Schaffer collaterals in the hippocampus of WT, *Drd1a*$^{-/-}$, WT-GFP, and *Drd1a*-siRNA mice, respectively. Scale bar, 50 μm.

Table 1. HFS-induced Egr1 expression in the hippocampus of alive mice

	Egr1-positive nuclei/mm^2			
	WT	*Drd1a*$^{-/-}$	WT-GFP	*Drd1a*-siRNA
Basal	103 ± 39	143 ± 78	341 ± 101	134 ± 103
HFS	1418 ± 106**	734 ± 124*#	1637 ± 112**	643 ± 163*# Δ

Quantification of HFS-induced Egr1 expression in hippocampal slices is shown. Immunostained cells were counted in hippocampal sections (examples in Fig. 9) obtained from different animals ($n = 12$ for each group). Numbers indicate immunostained nuclei per square millimeter (mean ± SEM).

*$p < 0.05$; **$p < 0.0005$ compared with the same group of animals in basal conditions. #$p < 0.01$ compared with HFS WT mice. Δ$p < 0.01$ compared with HFS WT-GFP mice. Statistics were determined by ANOVA followed by *post hoc* analysis with Tukey's test.

amygdala-dependent) fear conditioning, with relatively less impairment in amygdala-dependent learning. These data are consistent with our passive avoidance test results and complement our other findings. However, they contradict a previous study that found increased fear-induced freezing in *Drd1a*$^{-/-}$ mice (El-Ghundi et al., 2001). This discrepancy is likely caused by differences in methodology.

To study extinction, we increased the footshock intensity to achieve similar retention in both groups of mice. Under these conditions, we found no difference between WT and *Drd1a*$^{-/-}$ mice in extinction of fear conditioning, consistent with a previous report (El-Ghundi et al., 2001). The same report showed that using higher-intensity footshocks (two consecutive 0.9 mA, 3 s shocks; four times at 5 min intervals) significantly increased retention (El-Ghundi et al., 2001) in *Drd1a*$^{-/-}$ mice. Together, these studies suggest that with moderate intensity stimuli, D_1R are important for fear conditioning, but at higher intensities, D_1R-independent mechanisms predominate. Similar results were obtained with *Egr1* mutant mice, which exhibit deficits in spatial memory that can be rescued by extensive training (Jones et al., 2001).

It is widely accepted that hippocampal circuits are involved in the acquisition of classically conditioned eyelid responses (Berger et al., 1983; Thompson, 1988; Moyer et al., 1990; Gruart et al., 2006). Using unitary *in vivo* recordings, hippocampal pyramidal cell firing in response to CS presentations increases across conditioning sessions (McEchron and Disterhoft, 1997; Múnera et al., 2001; McEchron et al., 2003). Recently, it has been shown that trace eyeblink conditioning evokes a concomitant change in fEPSP strength at the hippocampal CA3–CA1 synapse in behaving mice (Gruart et al., 2006). We found that both acquisition of classically conditioned eyelid responses and the increase in CA3–CA1 synaptic strength across training are severely impaired in *Drd1a*$^{-/-}$ and *Drd1a*-siRNA mice, suggesting the D_1R plays an important role in hippocampal mechanisms related to learning and memory. These data support our previous finding that the D_1R is critical for certain forms of hippocampal synaptic plasticity *in vitro* (Granado et al., 2008). In addition, they also support the notion that learning and activity-dependent synaptic plasticity at the CA3–CA1 synapse are functionally related.

Both the generation of eyelid CRs and related changes in CA3–CA1 synaptic strength require a large number (>300) of paired CS-US presentations (Woody, 1986). In contrast, LTP is a fundamental property of most excitatory synapses in the mammalian brain that can be evoked by HFS of selected afferent pathways. Recent studies showed that trace eyeblink conditioning and the associated change in CA3–CA1 synaptic strength are prevented by HFS of the Schaffer collateral pathway, suggesting that the evoked LTP maximizes synaptic efficiency, occluding subsequent learning (Gruart et al., 2006). Moreover, learning-evoked changes in synaptic strength interfere with subsequent induction of LTP by HFS (Whitlock et al., 2006). Thus, these three processes (associative learning, activity-dependent synaptic plasticity, and LTP) seem to be functionally related (Gruart et al., 2006; Madroñal et al., 2007). In support of this, we found that D_1R are also necessary for evoking LTP of the CA3–CA1 synapse after HFS of afferent Schaffer collaterals. Since input–output curves and paired-pulse potentiation were normal in both *Drd1a*$^{-/-}$ and *Drd1a*-siRNA mice, we conclude that the D_1R does not affect normal transmission but contributes to synaptic plasticity during the acquisition and storage of new information.

We observed a marked reduction in Egr1 protein expression 24 h after *in vivo* tetanic stimulation of hippocampal CA3–CA1 in *Drd1a*$^{-/-}$ and *Drd1a*-siRNA mice. This inhibition is in agreement with the decrease in LTP in D_1R-depleted mice and indicates that hippocampal D_1R expression is necessary for these processes, consistent with results obtained in hippocampal slices from classical *Drd1a*$^{-/-}$ mice (Granado et al., 2008). Our results are consistent with previous data showing that inactivation of *Egr1* blocks long-term memory and LTP maintenance (Davis et al., 2000; Guzowski et al., 2000; Jones et al., 2001). In addition, the decrease in Egr1 expression after tetanic stimulation in *Drd1a*$^{-/-}$ indicates that the signaling mechanisms linking synaptic activation in dendrites with nuclear gene expression require D_1R activation in the hippocampus (Granado et al., 2008) and other brain areas including the striatum (Darmopil et al., 2009).

The mechanism by which D_1R mediates associative learning is not known. One possibility is that D_1R-triggered cAMP signaling phosphorylates CREB (cAMP response element-binding protein), which activates the histone acetyl transferase enzyme CREB-binding protein (Mayr et al., 2001; Alarcón et al., 2004),

inducing expression of immediate-early genes, including *Egr1* and *arc*, which play a crucial role in reference memory (Guzowski et al., 2000; Jones et al., 2001). Alternatively, D_1Rs could directly phosphorylate NMDA receptors or the protein kinase C ζ isoform in hippocampus and amygdala, potentiating and maintaining synaptic strength (Gardner et al., 2001; Impey et al., 2002; Kelleher et al., 2004; Sacktor, 2008; Yao et al., 2008) by increasing the influx of calcium induced by NMDA receptor activation, as occurs in prefrontal cortex neurons (Kruse et al., 2009). Direct interaction between D_1 and NMDA receptors within the plasma membrane of pyramidal neurons may also occur, since D_1R can physically interact with NR1 and NR2A subunits, modulating receptor trafficking (Lee et al., 2002; Pei et al., 2004; Fiorentini et al., 2006). Coactivation of both receptors increases the presence of GluR1 receptors and facilitates their incorporation into synapses in hippocampal neurons (Smith et al., 2005; Gao et al., 2006; Sacktor, 2008). It is also possible that D_1Rs are selectively activated by burst firing of dopamine neurons, mainly during the presentation of salient events (Zweifel et al., 2009).

This work contributes to our emerging understanding of dopamine system function in learning and memory by firmly establishing the critical role of the D_1R in associative learning and the endogenous synaptic potentiation that accompanies it. In addition, it strengthens the proposed functional link between learning, synaptic potentiation, and hippocampal *Egr1* expression.

References

Alarcón JM, Malleret G, Touzani K, Vronskaya S, Ishii S, Kandel ER, Barco A (2004) Chromatin acetylation, memory, and LTP are impaired in CBP+/− mice: a model for the cognitive deficit in Rubinstein-Taybi syndrome and its amelioration. Neuron 6:947–959.

Bahi A, Dreyer JL (2004) Cocaine-induced expression changes of axon guidance molecules in the adult rat brain. Mol Cell Neurosci 28:275–291.

Bahi A, Boyer F, Kafri T, Dreyer JL (2004a) CD81-induced behavioural changes during chronic cocaine administration: in vivo gene delivery with regulatable lentivirus. Eur J Neurosci 19:1621–1633.

Bahi A, Boyer F, Gumy C, Kafri T, Dreyer JL (2004b) In vivo gene delivery of urokinase-type plasminogen activator with regulatable lentivirus induces behavioural changes in chronic cocaine administration. Eur J Neurosci 20:3473–3488.

Baldwin AE, Sadeghian K, Kelley AE (2002) Appetitive instrumental learning requires coincident activation of NMDA and dopamine D1 receptors within the medial prefrontal cortex. J Neurosci 22:1063–1071.

Barnes CA (1979) Memory deficits associated with senescence: a neurophysiological and behavioral study in the rat. J Comp Physiol Psychol 93:74–104.

Berger TW, Rinaldi P, Weisz DJ, Thompson RF (1983) Single-unit analysis of different hippocampal cell types during classical conditioning of rabbit nictitating membrane response. J Neurophysiol 50:1197–1219.

Bliss TVP, Gardner-Medwin AR (1973) Long-lasting potentiation of synaptic transmission in the dentate area of the unanaesthetized rabbit following stimulation of the perforant path. J Physiol 232:357–374.

Crawley JN (2007) What's wrong with my mouse? Behavioral phenotyping of transgenic and knock out mice. Hoboken, NJ: Wiley.

Darmopil S, Martín AB, De Diego IR, Ares S, Moratalla R (2009) Genetic inactivation of dopamine D1 but not D2 receptors inhibits L-DOPA-induced dyskinesia and histone activation. Biol Psychiatry 6:603–613.

Darvas M, Palmiter RD (2009) Restriction of dopamine signaling to the dorsolateral striatum is sufficient for many cognitive behaviors. Proc Natl Acad Sci U S A 106:14664–14669.

Davis S, Vanhoutte P, Pages C, Caboche J, Laroche S (2000) The MAPK/ERK cascade targets both Elk-1 and cAMP response element-binding protein to control long-term potentiation-dependent gene expression in the dentate gyrus in vivo. J Neurosci 20:4563–4572.

Dreyer JL (2010) Lentiviral vector-mediated gene transfer and RNA silencing technology in neuronal dysfunctions. Methods Mol Biol 614:3–35.

Dubois B, Pillon B (1997) Cognitive deficits in Parkinson's disease. J Neurol 244:2–8.

El-Ghundi M, Fletcher PJ, Drago J, Sibley DR, O'Down BF, George SR (1999) Spatial learning deficit in dopamine D1 receptor knockout mice. Eur J Pharmacol 383:95–106.

El-Ghundi M, O'Dowd BF, George SR (2001) Prolonged fear responses in mice lacking dopamine D1 receptor. Brain Res 892:86–93.

Fiorentini C, Rizzetti MC, Busi C, Bontempi S, Collo G, Spano P, Missale C (2006) Loss of synaptic D1 dopamine/N-methyl-D-aspartate glutamate receptor complexes in L-DOPA-induced dyskinesia in the rat. Mol Pharmacol 69:805–812.

Gao C, Sun X, Wolf ME (2006) Activation of D1 dopamine receptors increases surface expression of AMPA receptors and facilitates their synaptic incorporation in cultured hippocampal neurons. J Neurochem 5:1664–1677.

Gardner B, Liu ZF, Jiang D, Sibley DR (2001) The role of phosphorylation/dephosphorylation in agonist-induced desensitization of D1 dopamine receptor function: evidence for a novel pathway for receptor dephosphorylation. Mol Pharmacol 59:310–321.

Granado N, Ortiz O, Suárez LM, Martín ED, Ceña V, Solís JM, Moratalla R (2008) D1 but not D5 dopamine receptors are critical for LTP, spatial learning, and LTP-Induced arc and zif268 expression in the hippocampus. Cereb Cortex 18:1–12.

Grande C, Zhu H, Martín AB, Lee M, Ortíz O, Hiroi N, Moratalla R (2004) Chronic treatment with atypical neuroleptics induces striosomal FosB/DeltaFosB expression in rats. Biol Psychiatry 55:457–463.

Gruart A, Blázquez P, Delgado-García JM (1995) Kinematics of unconditioned and conditioned eyelid movements in the alert cat. J Neurophysiol 74:226–248.

Gruart A, Muñoz MD, Delgado-García JM (2006) Involvement of the CA3–CA1 synapse in the acquisition of associative learning in behaving mice. J Neurosci 26:1077–1087.

Gureviciene I, Ikonen S, Gurevicius K, Sarkaki A, van Groen T, Pussinen R, Ylinen A, Tanila H (2004) Normal induction but accelerated decay of LTP in APP + PS1 transgenic mice. Neurobiol Dis 15:188–195.

Guzowski JF, Lyford GL, Stevenson GD, Houston FP, McGaugh JL, Worley PF, Barnes CA (2000) Inhibition of activity-dependent arc protein expression in the rat hippocampus impairs the maintenance of long-term potentiation and the consolidation of long-term memory. J Neurosci 20:3993–4001.

Hall J, Thomas KL, Everitt BJ (2001) Cellular imaging of Egr1 expression in the hippocampus and amygdala during contextual and cued fear memory retrieval: selective activation of hippocampal CA1 neurons during the recall of contextual memories. J Neurosci 21:2186–2193.

Harrison FE, Hosseini AH, McDonald MP (2009) Endogenous anxiety and stress responses in water maze and Barnes maze spatial memory tasks. Behav Brain Res 198247–198251.

Impey S, Fong AL, Wang Y, Cardinaux JR, Fass DM, Obrietan K, Wayman GA, Storm DR, Soderling TR, Goodman RH (2002) Phosphorylation of CBP mediates transcriptional activation by neural activity and CaM kinase IV. Neuron 34:235–244.

Jones MW, Errington ML, French PJ, Fine A, Bliss TV, Garel S, Charnay P, Bozon B, Laroche S, Davis S (2001) A requirement for the immediate early gene Egr1 in the expression of late LTP and long-term memories. Nat Neurosci 4:289–296.

Kelleher RJ 3rd, Govindarajan A, Jung HY, Kang H, Tonegawa S (2004) Translational control by MAPK signaling in long-term synaptic plasticity and memory. Cell 116:467–479.

Kelly MP, Deadwyler SA (2003) Experience-dependent regulation of the immediate-early gene arc differs across brain regions. J Neurosci 23:6443–6451.

Kruse MS, Prémont J, Krebs MO, Jay TM (2009) Interaction of dopamine D1 with NMDA NR1 receptors in rat prefrontal cortex. Eur Neuropsychopharmacol 19:296–304.

Kugelberg E (1952) Facial reflexes. Brain 75:385–396.

Lee FJ, Xue S, Pei L, Vukusic B, Chery N, Wang Y, Wang YT, Niznik HB, Yu XM, Liu F (2002) Dual regulation of NMDA receptor functions by direct protein-protein interactions with the dopamine D1 receptor. Cell 18:219–230.

Levin BE, Katzen HL (2005) Early cognitive changes and nondementing behavioral abnormalities in Parkinson's disease. Adv Neurol 98:84–94.

Li S, Cullen WK, Anwyl R, Rowan MJ (2003) Dopamine-dependent facilitation of LTP induction in hippocampal CA1 by exposure to spatial novelty. Nat Neurosci 6:526–531.

Lisman JE, Grace AA (2005) The hippocampal-VTA loop: controlling the entry of information into long-term memory. Neuron 46:703–713.

Madroñal N, Delgado-García JM, Gruart A (2007) Differential effects of long-term potentiation evoked at the CA3–CA1 synapse before, during, and after the acquisition of classical eyeblink conditioning in behaving mice. J Neurosci 27:12139–12146.

Madroñal N, Gruart A, Delgado-García JM (2009) Differing presynaptic contributions to LTP and associative learning in behaving mice. Front Behav Neurosci 3:7.

Mayr BM, Canettieri G, Montminy MR (2001) Distinct effects of cAMP and mitogenic signals on CREB-binding protein recruitment impart specificity to target gene activation via CREB. Proc Natl Acad Sci U S A 98:10936–10941.

McEchron MD, Disterhoft JF (1997) Sequence of single neuron changes in CA1 hippocampus of rabbits during acquisition of trace eyeblink conditioned responses. J Neurophysiol 78:1030–1044.

McEchron MD, Tseng W, Disterhoft JF (2003) Single neurons in CA1 hippocampus encode trace interval duration during trace heart rate (fear) conditioning in rabbit. J Neurosci 23:1535–1547.

McIntyre CK, Miyashita T, Setlow B, Marjon KD, Steward O, Guzowski JF, McGaugh JL (2005) Memory-influencing intra-basolateral amygdala drug infusions modulate expression of Arc protein in the hippocampus. Proc Natl Acad Sci U S A 102:10718–10723.

Moratalla R, Xu M, Tonegawa S, Graybiel AM (1996) Cellular responses to psychomotor stimulant and neuroleptic drugs are abnormal in mice lacking the D1 dopamine receptor. Proc Natl Acad Sci U S A 93:14928–14933.

Moyer JRJ, Deyo RA, Disterhoft JF (1990) Hippocampectomy disrupts trace eye-blink conditioning in rabbits. Behav Neurosci 104:243–252.

Mühlbauer M, Allard B, Bosserhoff AK, Kiessling S, Herfarth H, Rogler G, Schömerich J, Jobin C, Hellerbrand C (2004) Differential effects of deoxycholic acid and taurodeoxycholic acid on NF-κB signal transduction and IL-8 gene expression in colonicepithelial cells. Am J Physiol Gastrointest Liver Physiol 286:G1000–G1008.

Múnera A, Gruart A, Muñoz MD, Fernández-Más R, Delgado-García JM (2001) Discharge properties of identified CA1 and CA3 hippocampus neurons during unconditioned and conditioned eyelid responses in cats. J Neurophysiol 86:2571–2582.

O'Carroll CM, Morris RG (2004) Heterosynaptic co-activation of glutamatergic and dopaminergic afferents is required to induce persistent long-term potentiation. Neuropharmacology 47:324–332.

O'Carroll CM, Martin SJ, Sandin J, Frenguelli B, Morris RG (2006) Dopaminergic modulation of the persistence of one-trial hippocampus-dependent memory. Learn Mem 13:760–769.

Otmakhova NA, Lisman JE (1996) D1/D5 dopamine receptor activation increases the magnitude of early long-term potentiation at CA1 hippocampal synapses. J Neurosci 16:7478–7486.

Palmiter RD (2008) Dopamine signaling in the dorsal striatum is essential for motivated behaviors: lessons from dopamine-deficient mice. Ann N Y Acad Sci 1129:35–46.

Patil SS, Sunyer B, Höger H, Lubec G (2009) Evaluation of spatial memory of C57BL/6J and CD1 mice in the Barnes maze, the Multiple T-maze and in the Morris water maze. Behav Brain Res 198:58–68.

Pavón N, Martín AB, Mendialdua A, Moratalla R (2006) ERK phosphorylation and FosB expression are associated with L-DOPA-induced dyskinesia in hemiparkinsonian mice. Biol Psychiatry 59:64–74.

Paxinos G, Franklin KBJ (2001) The mouse brain in stereotaxic coordinates. London: Academic.

Pei L, Lee FJ, Moszczynska A, Vukusic B, Liu F (2004) Regulation of dopamine D1 receptor function by physical interaction with the NMDA receptors. J Neurosci 4:1149–1158.

Pittenger C, Fasano S, Mazzocchi-Jones D, Dunnett SB, Kandel ER, Brambilla R (2006) Impaired bidirectional synaptic plasticity and procedural memory formation in striatum-specific cAMP response element-binding protein-deficient mice. J Neurosci 10:2808–2813.

Porras-García E, Cendelin J, Domínguez-del-Toro E, Vožeh F, Delgado-García JM (2005) Purkinje cell loss affects differentially the execution, acquisition and prepulse inhibition of skeletal and facial motor responses in Lurcher mice. Eur J Neurosci 21:979–988.

Ramiro-Fuentes S, Ortiz O, Moratalla R, E Fernandez-Espejo (2010) Intra-accumbal rimonabant is rewarding but induces aversion to cocaine in cocaine-treated rats, as does in vivo CB1R silencing: critical role for glutamate receptors. Neuroscience 167:205–215.

Rivera A, Alberti I, Martin AB, Narvaez JA, de la Calle A, Moratalla R (2002) Molecular phenotype of rat striatal neurons expressing the dopamine D5 receptor subtype. Eur J Neurosci 16:2049–2058.

Rossato JI, Bevilaqua LR, Izquierdo I, Medina JH, Cammarota M (2009) Dopamine controls persistence of long-term memory storage. Science 325:1017–1020.

Sacktor TC (2008) PKMzeta, LTP maintenance, and the dynamic molecular biology of memory storage. Prog Brain Res 169:27–40.

Shannon HE, Hart JC, Bymaster FP, Calligaro DO, DeLapp NW, Mitch CH, Ward JS, Fink-Jensen A, Sauerberg P, Jeppesen L, Sheardown MJ, Swedberg MD (1999) Muscarinic receptor agonists, like dopamine receptor antagonist antipsychotics, inhibit conditioned avoidance response in rats. J Pharmacol Exp Ther 290:901–907.

Smith DR, Striplin CD, Geller AM, Mailman RB, Drago J, Lawler CP, Gallagher M (1998) Behavioural assessment of mice lacking D1A dopamine receptors. Neuroscience 86:135–146.

Smith JW, Fetsko LA, Xu R, Wang Y (2002) Dopamine D2L receptor knockout mice display deficits in positive and negative reinforcing properties of morphine and in avoidance learning. Neuroscience 113:755–765.

Smith WB, Starck SR, Roberts RW, Schuman EM (2005) Dopaminergic stimulation of local protein synthesis enhances surface expression of GluR1 and synaptic transmission in hippocampal neurons. Neuron 3:765–779.

Smith-Roe SL, Kelley AE (2000) Coincident activation of NMDA and dopamine D1 receptors within the nucleus accumbens core is required for appetitive instrumental learning. J Neurosci 20:7737–7742.

Takatsuki K, Kawahara S, Kotani S, Fukunaga S, Mori H, Mishina M, Kirino Y (2003) The hippocampus plays an important role in eyeblink conditioning with a short trace interval in glutamate receptor subunit delta 2 mutant mice. J Neurosci 23:17–22.

Thompson RF (1988) The neural basis of basic associative learning of discrete behavioral responses. Trends Neurosci 11:152–155.

Viosca J, Lopez de Armentia M, Jancic D, Barco A (2009) Enhanced CREB-dependent gene expression increases the excitability of neurons in the basal amygdala and primes the consolidation of contextual and cued fear memory. Learm Mem 16:193–197.

Whishaw IQ, Dunnett SB (1985) Dopamine depletion, stimulation or blockade in the rat disrupts spatial navigation and locomotion dependent upon beacon or distal cues. Behav Brain Res 18:11–29.

Whitlock JR, Heynen AJ, Shuler MG, Bear MF (2006) Learning induces long-term potentiation in the hippocampus. Science 313:1093–1097.

Williams GV, Goldman-Rakic PS (1995) Modulation of memory fields by dopamine D1 receptors in prefrontal cortex. Nature 376:572–575.

Woody CD (1986) Understanding the cellular basis of memory and learning. Annu Rev Psychol 37:433–493.

Xu M, Moratalla R, Gold LH, Hiroi N, Koob GF, Graybiel AM, Tonegawa S (1994) Dopamine D1 receptor mutant mice are deficient in striatal expression of dynorphin and in dopamine-mediated behavioral responses. Cell 79:729–742.

Yao Y, Kelly MT, Sajikumar S, Serrano P, Tian D, Bergold PJ, Frey JU, Sacktor TC (2008) PKM zeta maintains late long-term potentiation by *N*-ethylmaleimide-sensitive factor/GluR2-dependent trafficking of postsynaptic AMPA receptors. J Neurosci 28:7820–7827.

Zheng JF, Patil SS, Chen WQ, An W, He JQ, Höger H, Lubec G (2009) Hippocampal protein levels related to spatial memory are different in the Barnes maze and in the multiple T-maze. J Proteome Res 8:4479–4486.

Zweifel LS, Parker JG, Lobb CJ, Rainwater A, Wall VZ, Fadok JP, Darvas M, Kim MJ, Mizumori SJ, Paladini CA, Phillips PE, Palmiter RD (2009) Disruption of NMDAR-dependent burst firing by dopamine neurons provides selective assessment of phasic dopamine-dependent behavior. Proc Natl Acad Sci U S A 106:7281–7288.